NUREG/CR--4667-Vol.5

TI89 008096

NUREG/CR-4667
ANL-88-32
Vol. V
R5

Environmentally Assisted Cracking in Light Water Reactors

Semiannual Report
April - September 1987

Manuscript Completed: June 1988
Date Published: February 1989

Prepared by
W.J. Shack, T.F. Kassner, P.S. Maiya,
J.Y. Park, W.E. Ruther

Argonne National Laboratory
9700 South Cass Avenue
Argonne, IL 60439

Prepared for
Division of Engineering
Office of Nuclear Regulatory Research
U.S. Nuclear Regulatory Commission
Washington, DC 20555
NRC FIN A2212

Previous Documents in Series

Environmentally Assisted Cracking in Light Water Reactors Annual Report October 1983–September 1984, NUREG/CR-4287, ANL-85-33 (June 1985).

Light-Water-Reactor Safety Materials Engineering Research Programs: Quarterly Progress Report October—December 1984, NUREG/CR-3998 Vol. III, ANL-84-60 Vol. III (October 1985).

Light-Water-Reactor Safety Materials Engineering Research Programs: Quarterly Progress Report January—March 1985, NUREG/CR-4490 Vol. I, ANL-85-75 Vol. I (March 1986).

Environmentally Assisted Cracking in Light Water Reactors Semiannual Report April—September 1985, NUREG/CR-4667 Vol. I, ANL-86-31 (June 1986).

Environmentally Assisted Cracking in Light Water Reactors Semiannual Report October 1985—March 1986, NUREG/CR-4667 Vol. II, ANL-86-37 (September 1987).

Environmentally Assisted Cracking in Light Water Reactors Semiannual Report April—September 1986, NUREG/CR-4667 Vol. III, ANL-87-37 (September 1987).

Environmentally Assisted Cracking in Light Water Reactors Semiannual Report October 1986—March 1987, NUREG/CR-4667 Vol. IV, ANL-87-41 (December 1987).

Environmentally Assisted Cracking in Light Water Reactors

by

W. J. Shack, T. F. Kassner, P. S. Maiya,
J. Y. Park, and W. E. Ruther

Abstract

This report summarizes work performed by Argonne National Laboratory on environmentally assisted cracking in light water reactors during the six months from April to September 1987. The stress corrosion cracking (SCC) behavior of Types 304, 316NG, and 347 stainless steel (SS) was investigated by means of slow-strain-rate and fracture-mechanics crack-growth-rate tests in high-temperature water. The relative susceptibility of the solution-annealed Type 304 SS to crack initiation was determined in water with two dissolved-oxygen concentrations. The effect of dissolved copper and organic impurities on the SCC of sensitized Type 304 SS was also investigated. Fatigue tests are being conducted on Type 316NG SS in air at room temperature to provide baseline data for comparison with results that will be obtained in high-temperature water. The susceptibility of several heats of different grades of low-alloy steel to transgranular SCC was explored in slow-strain-rate tests at 289°C, and the variation in the crack growth rates was attributed to differences in the sulfur content and sulfide inclusion distributions in the materials.

Contents

List of Figures

List of Tables

Executive Summary

Fracture-mechanics crack-growth tests were performed to determine the effect of water flow rate on the stress corrosion cracking (SCC) behavior of Type 316NG SS at 289°C. In one phase of the tests, water was directed across the mouth of the crack in a "high-flow" specimen by means of a high-velocity pump, whereas the flow past an identical "low-flow" specimen was due only to recirculation of the water within the autoclave. In another phase, a low "quasi-static" flow past both specimens was maintained by thermal convection and the refreshment rate of the water within the autoclave. No crack growth occurred in the "high-flow" specimen over a time period of ~6400 h under any water chemistry or flow conditions. The crack growth rate of the "low-flow" specimen was consistent with values determined previously for this material under similar water chemistry and loading conditions. The results of this experiment imply that the high flow velocity of water past the mouth of the fatigue crack in the 1T compact-tension specimen prevented SCC initiation. Consequently, no information was obtained on the influence of flow velocity on crack propagation under high- and low-flow rate conditions.

Fracture-mechanics crack-growth tests were also performed to compare the SCC behavior of Types 316NG and CF3M cast SS in oxygenated water under low-frequency, cyclic loading at 289°C. No crack growth occurred in either specimen over a time period of ~740 h. The test was terminated shortly thereafter because of problems with the equipment.

Constant-extension-rate tensile (CERT) tests were performed to evaluate heat-to-heat variations in the SCC susceptibility of Types 316NG and 347 SS in oxygenated water (0.2 ppm) containing 0.1 ppm sulfate, at 289°C and strain rates between 10^{-6} and 10^{-7} s^{-1}. In terms of the critical strain rate, i.e., the strain rate at or below which SCC occurs in the steels, Type 316NG SS is more resistant to SCC than sensitized Types 304 or 316 SS, and Type 347 SS is somewhat more resistant than Type 316NG SS in terms of this measure of resistance to SCC. No correlation was found between the SCC behavior and the minor variations in chemical composition among the different heats of the steels. However, a significant effect of heat treatment was observed. A heat of Type 347 SS that susceptible to TGSCC in the solution-annealed condition is becomes extremely resistant to SCC in the aged condition. Although no sensitization occurred in either condition, differences in precipitate structure in the materials due to the different heat treatments appear to influence the SCC behavior. This observation can be rationalized in terms of the effect of niobium in the solution-annealed material on the stacking fault energy, and the nature of slip processes in the solution-annealed and aged materials.

Baseline fatigue tests were performed on Type 316NG SS in air at room temperature for comparison with the ASME Section III design curve and the ASME mean data curve. The results agree well with the mean data curve for fairly short lives corresponding to plastic strain ranges greater than 0.5%, but fall below the mean data curve at longer lives. Similar fatigue tests will be performed in high-temperature water to assess the effect of simulated BWR and PWR environments on the design margin or safety factor incorporated into the ASME mean life curve for austenitic stainless steels.

Metallic impurities (viz., corrosion products) from the feedwater train are present in reactor coolant water along with the various ionic species that enter the

coolant from leaks and other sources. In plants with admiralty brass, aluminum brass, or copper–nickel condenser tubes and/or feedwater heaters, copper (e.g., CuO or Cu_2O) and iron can dissolve in high–temperature water. Previous work indicated that the minimum concentration of Cu^{2+} required for severe IGSCC of sensitized Type 304 SS decreased from ~1.0 ppm at 289°C to ~0.1 ppm at 150°C. These concentrations are higher than those typically encountered in the reactor coolant water in BWRs and in secondary system water of recirculating or once–through steam generators in PWRs. However, since the thermodynamic stability regime of Cu^{+} increases at the expense of Cu^{2+} as the temperature of the water increases, a series of CERT experiments was performed to determine the minimum concentration of Cu^{+} in low–oxygen water for SCC of sensitized Type 304 SS at temperatures between 135 and 289°C. The results indicate that SCC occurs at and above ~1 ppm Cu^{+} at 289°C, i.e., the same concentration as Cu^{2+}; however, at temperatures below ~200°C, SCC occurs at lower concentrations of Cu^{+} (~0.03 ppm). The temperature dependence of the crack growth rates in deoxygenated water containing 1–2 ppm Cu^{+} revealed a broad maximum between ~170 and 250°C with a decrease in the rates at higher and lower temperatures, which is similar to the SCC behavior in high–purity water containing 0.2 ppm dissolved oxygen. However, the crack growth rates in deoxygenated water with dissolved copper were higher by a factor of 10. The effect of pH on the SCC susceptibility in the presence of dissolved copper is being investigated.

Organic contaminants can enter BWR reactor coolant and PWR secondary–system water in a variety of ways. As part of an investigation of the effects of organic acids on SCC, CERT tests were performed on sensitized Type 304 SS in water at 289°C containing 0.2 ppm dissolved oxygen and four EDTA salts at an anion concentration of 1 ppm. Transgranular SCC was observed but the crack growth rates were very low, primarily because these substances react with the dissolved oxygen and decrease the concentration to <5 ppb in the effluent water with a concomitant decrease in the open–circuit electrochemical potential (ECP) of the steel to less than –500 mV(SHE).

Previous studies of crack initiation in Type 316NG SS and solution–annealed and sensitized Type 304 SS indicated that crack initiation occurs at local plastic strains of ~2 to 4% in water containing ~0.2 ppm dissolved oxygen and 0.1 ppm sulfate at 289°C. CERT experiments have been performed on solution–annealed Type 304 SS to determine whether resistance to initiation of transgranular cracks is greater in low–oxygen (<5 ppb) water. The results showed that even at ECP values of less than –400 mV(SHE), cracks initiate at strains of ~4%. Also, the crack growth rates of the steel in the two environments were virtually the same.

CERT tests were performed on a variety of ferritic steels used for LWR pressure vessels and primary system piping. Virtually all of the materials exhibited TGSCC in water containing ~0.2 ppm dissolved oxygen and 0.1 ppm sulfate at 289°C. However, the crack growth rates varied over a wide range (e.g., 10^{-10} to 10^{-8} s^{-1}), even for the same heat of material. This variation among the different grades of steel and for the same heat of steel was attributed to the sulfur content and distribution, i.e., materials with fewer sulfide inclusions were less susceptible to TGSCC.

1
Introduction

The objective of this program is to develop an independent capability for the assessment of environmentally assisted cracking in light water reactor (LWR) systems. During this reporting period, the program has been primarily directed at problems of intergranular stress corrosion cracking (IGSCC). The scope of the work includes (1) evaluation of the influence of metallurgical variables, stress, and the environment on susceptibility to stress corrosion cracking (SCC), including the influence of plant operations on these variables; and (2) examination of practical limits for these variables to effectively control SCC in LWR systems.

The effort during this reporting period has focused on (1) an evaluation of the SCC of alternative materials, (2) an investigation of the effects of water chemistry on the SCC of sensitized Type 304 SS, and (3) an investigation of environmentally assisted cracking of ferritic steels. The program seeks to evaluate potential solutions to SCC in LWRs by direct experimentation, through the development of a better understanding of the various phenomena.

2
Alternative Materials

2.1
Introduction

The objective of this work is to evaluate the resistance of Types 316NG, 347, and CF-3 stainless steel (SS) to environmentally assisted cracking in simulated BWR water. These alternative materials for recirculation system piping in BWRs are very resistant to sensitization, and thus are much less susceptible to IGSCC than the Types 304 and 316 SS used in many operating reactors in the U.S. However, their resistance to other modes of degradation such as transgranular stress corrosion cracking (TGSCC) and corrosion-assisted fatigue must be evaluated over the wide range of water chemistries encountered in reactor-coolant systems.

Fracture mechanics tests were performed on Type 316NG SS to develop a more extensive data base for crack growth rates in this material and to better understand the effects of water flow rate on crack growth. CERT tests were performed on Type 347 SS to evaluate the effects of heat treatment on susceptibility to TGSCC. Although the heat treatments do not produce sensitization, variations in the precipitate structure do appear to influence susceptibility to TGSCC.

2.2
Technical Progress

2.2.1
Fracture Mechanics Crack Growth Tests (W. E. Ruther, W. K. Soppet, J. Y. Park, and T. F. Kassner)

Influence of Flow Rate on Type 316NG SS in 289°C Water

Fracture-mechanics crack-growth-rate tests were performed to determine the effect of water flow rate on the SCC behavior of Type 316NG SS (Heat No. P91576) in high-purity water with 0.2-0.3 ppm dissolved oxygen and in water containing 0.1 ppm of either nitrate or sulfate at this oxygen concentration. As in previous tests, the specimens were fatigue-precracked in air at 289°C to provide 1-mm-deep starter cracks before testing in water at this temperature. A schematic of the system in which the tests were performed is shown in Fig. 1. Under high-flow-rate conditions, the water was recirculated in the autoclave at a rate of ~0.5 $L \cdot s^{-1}$ by means of a high-temperature, high-pressure canned rotor

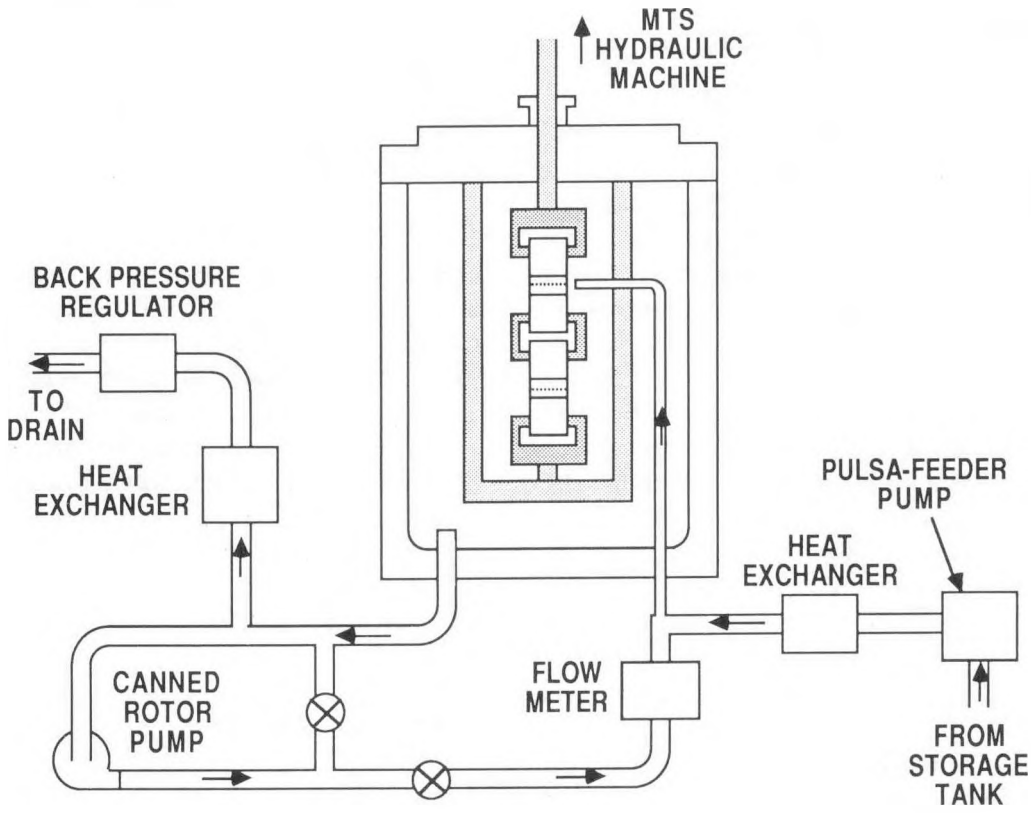

Figure 1. Schematic of Autoclave System for Investigating the Effect of Water Flow Rate on Crack Growth in Fracture-Mechanics-Type Specimens of Stainless Steels under Low-Frequency Cyclic Loading.

pump. The water was directed across the mouth of the crack in the upper specimen by means of a 10-mm-diam orifice positioned as shown in Figs. 1 and 2; this specimen was designated the high-flow-velocity (HFV) specimen. When the recirculation pump was in operation, the flow velocity at the orifice was ~6.4 $m \cdot s^{-1}$. A Pulsa-feeder pump continuously injected feedwater into the system at a rate of ~1.7 x 10^{-4} $L \cdot s^{-1}$ (10 $cm^3 \cdot min^{-1}$) to maintain the dissolved-oxygen concentration in the water at the 0.2 to 0.3-ppm level. When the recirculation pump was not in operation, the flow velocity at the orifice due to the injected feedwater was ~0.002 $m \cdot s^{-1}$. No flow was directed across the crack mouth of the lower specimen, which was designated the low-flow-velocity (LFV) specimen; however, the linear flow velocity of water in the autoclave was ~0.05 $m \cdot s^{-1}$ when the recirculation pump was in operation. Thermal convection plus the flow owing to the refreshment rate of water in the autoclave produced the normal "quasi-static" condition of water flow past both specimens in one phase of the test. The tests were conducted under low-frequency, cyclic loading with a positive sawtooth waveform at a frequency of 8 x 10^{-2} Hz and an R value of 0.95. The stress intensity factors ranged from about 27 to 34 $MPa \cdot m^{1/2}$. Crack growth was determined from compliance measurements by means of MTS clip gages attached to the specimens.

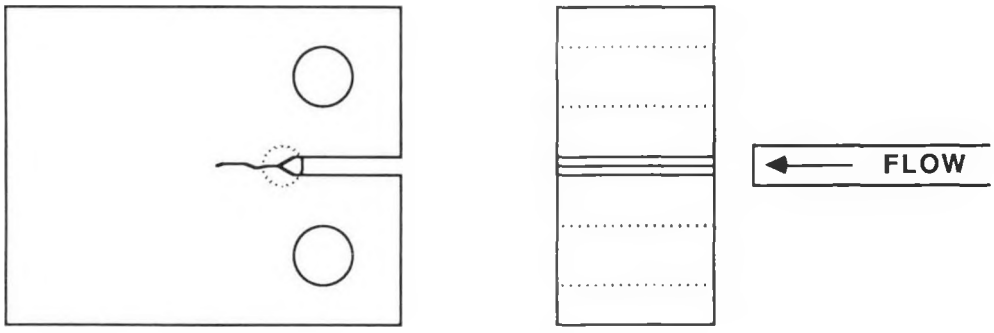

Figure 2. Orientation of Flow Orifice in Relation to the Fatigue Crack in the "High-Flow-Velocity" 1T Compact Tension Specimen.

The results, shown in Table 1, indicate that no crack growth occurred in the HFV specimen under any of the water chemistry and flow conditions over a time period of ~6400 h. During test periods 1 and 3–5, the recirculation pump was in operation, and during test period 2, the pump was turned off to decrease the flow velocity past the crack mouth of this specimen. As indicated in the table, crack growth did not initiate in this specimen during the ~1000-h period under the low-flow condition.

In contrast, the crack growth rate in the LFV specimen was 3×10^{-10} and $\sim 1 \times 10^{-10}$ $m \cdot s^{-1}$ in high-purity water during test periods 1 and 3, respectively. The crack growth rate when 0.1 ppm of either nitrate or sulfate was added to the feedwater (periods 4 and 5) was $\sim 8 \times 10^{-11}$ $m \cdot s^{-1}$. These values are in excellent agreement with previous results on this material under the same water chemistry conditions.[1] The crack growth rate of the LFV specimen was lower by approximately one order of magnitude during test period 2, in which the recirculation pump was turned off. At present, we have no explanation for this result: however, the decrease in the crack growth rate cannot be attributed to a low dissolved-oxygen concentration in the water since the electrochemical potential (ECP) of the stainless steel was ~80 mV(SHE) and the effluent oxygen concentration remained in the 0.2 to 0.3-ppm range.

The observation that the specimen exposed to a high-velocity flow of water across the crack mouth did not undergo SCC may be attributed to the absence of a macrocell corrosion process between the mouth and tip of the crack under this condition. In other words, the water chemistry at the crack tip was similar to that in the bulk solution, in contrast to the conditions at the tip of an active stress corrosion crack, where acidification and deoxygenation of the water facilitate anodic dissolution of the metal during repeated film rupture events.

Figure 3 shows the morphology of the fatigue and stress corrosion cracks in the two specimens in which the effect of the water flow rate on SCC was explored. The compact tension (1TCT) specimens were sectioned vertically, and half of each specimen was split in the plane of the crack at liquid nitrogen temperature to reveal the fracture surface. The corrosion-product film was removed from the fracture surface by the APAC process[2,3] [i.e., by exposure of the specimens for 2 h in a gently boiling alkaline permanganate solution (20% NaOH, 3% $KMnO_4$), followed by a hot rinse

Table 1. Crack Growth Results for Two Type 316NG SS Specimens[a] during an Experiment[b] at 289°C in Which the Flow Rate of Water in the Autoclave Was Altered to Change the Flow Past the Specimens

Test Period	Interval, h	Overall Flow Rate,[c] $L \cdot s^{-1}$	Cond., µS/cm	Electrode Potentials mV(SHE)		Results for HFV Specimen[d]		Results for LFV Specimen[e]	
				304 SS	Pt	K_{max},[f] $MPa \cdot m^{1/2}$	$\dot{a}_{av}$, $m \cdot s^{-1}$	K_{max},[f] $MPa \cdot m^{1/2}$	$\dot{a}_{av}$, $m \cdot s^{-1}$
1	0–1707	0.5	0.13	75	--	27.2	~0	32.1	3.0×10^{-10}
2	1707–2884	0.01	0.12	80	85	27.2	~0	32.2	2.5×10^{-11}
3	2884–4273	0.5	0.15	140[g]	160[g]	27.2	~0	33.2	1.1×10^{-10}
4	4273–5379	0.5	0.77[h]	200[g]	215[g]	27.2	~0	33.7	8.4×10^{-11}
5	5379–6387	0.5	0.80[i]	190	220	27.2	~0	34.4	7.9×10^{-11}

[a] Compact tension specimens (1TCT) of Type 316NG SS (Heat No. P91576) received the following heat treatment: solution anneal at 1050°C for 0.5 h plus 650°C for 24 h (EPR = 0 C/cm^2).

[b] Frequency and load ratio, R, for the positive sawtooth waveform were 8×10^{-2} Hz and 0.95, respectively. Effluent dissolved-oxygen concentration was 0.2–0.3 ppm.

[c] High-pressure, high-temperature recirculation pump operated during test periods 1 and 3-5; thermal convection coupled with the refreshment flow rate of 0.6 $L \cdot h^{-1}$ ($\sim 1.7 \times 10^{-4}$ $L \cdot s^{-1}$) provided flow during test period 2.

[d] Local flow velocity at crack mouth was ~6.4 $m \cdot s^{-1}$ during test periods 1 and 3-5, and ~0.002 $m \cdot s^{-1}$ during test period 2.

[e] No flow directed across crack mouth; linear flow velocity in the autoclave was ~0.05 $m \cdot s^{-1}$ during test periods 1 and 3-5.

[f] Stress intensity value at the end of the test period.

[g] Electrolyte in the reference electrode was replaced for this segment of the experiment.

[h] HNO_3 (0.12 ppm) added to the feedwater.

[i] H_2SO_4 (0.10 ppm) added to the feedwater.

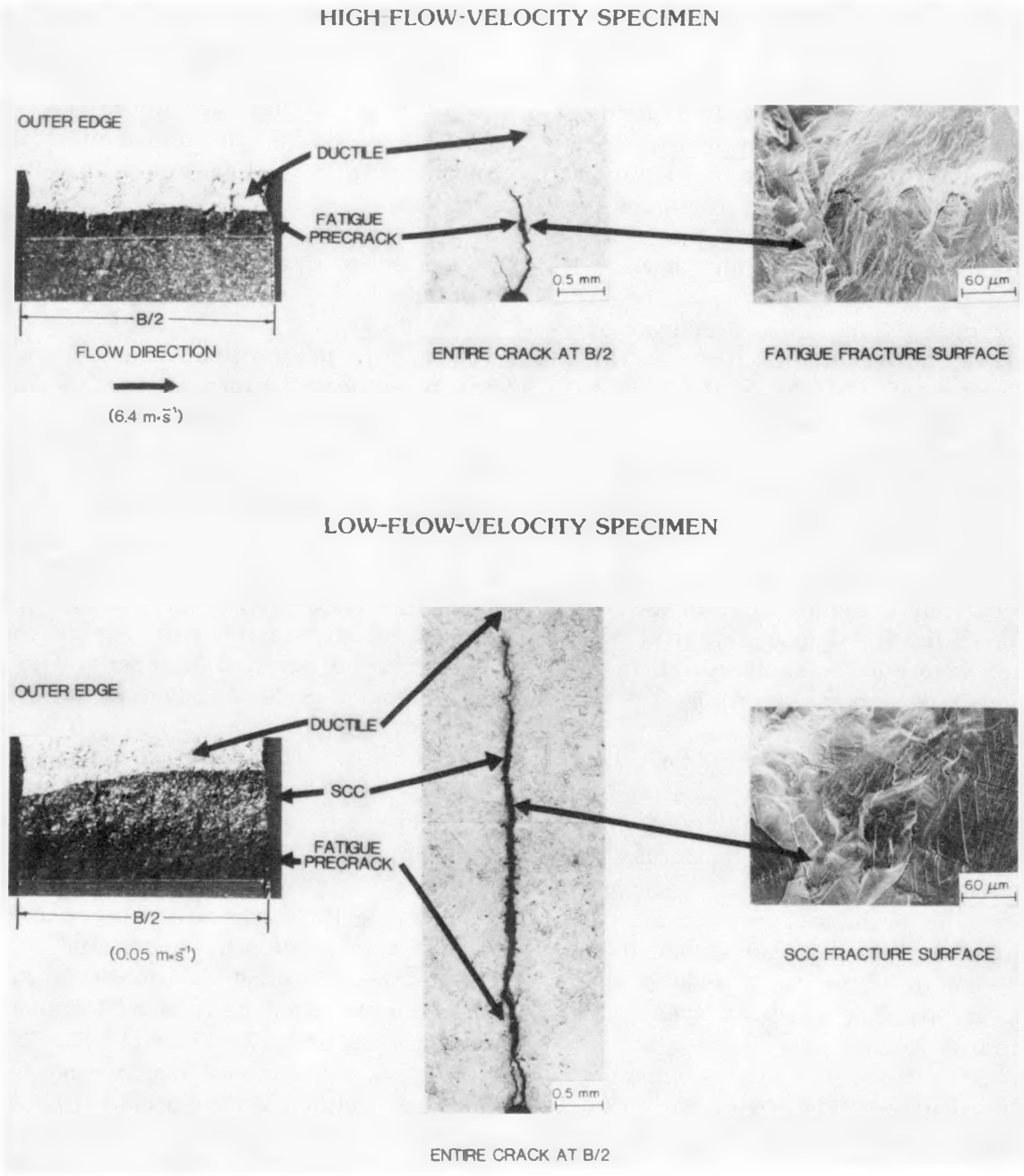

Figure 3. Micrographs of the Initial Fatigue Crack in the "High-Flow-Velocity" Specimen (No. E02) and the Transgranular Stress Corrosion Crack in the "Low-Flow-Velocity" Specimen (No. E03) of Type 316NG SS (Heat No. P91576) after Simultaneous Exposure to Low-Frequency Cyclic Loading under Simulated BWR Water Chemistry Conditions at 289°C.

and then 2 h in a dibasic ammonium citrate solution] to reveal the morphology of the underlying material. The intact portion of the specimen that encompassed the crack was polished and etched to corroborate the mode of crack propagation and also to determine if macrobranching of the crack had occurred during the test. In addition, the total crack lengths at the end of the tests were measured and compared with the values obtained from the clip gages.

The micrographs in Fig. 3 indicate that the crack path and fracture surface morphology of the Type 316NG SS specimen exposed to a low flow velocity was transgranular, as in previous specimens.[4] TGSCC is invariably the mode of crack propagation in this material during CERT experiments.[5,6] In the LFV specimen, the crack front progressed uniformly from the outer edge to the half-thickness (B/2) of the material with minimal edge effects, as indicated in the lower left-hand photograph in Fig. 3.

The micrographs of the crack front and the polished section of the Type 316NG SS specimen subjected to a relatively high flow velocity across the crack mouth indicate that no SCC occurred from the base of the fatigue precrack. This is consistent with the compliance measurements of the crack length, which also indicated that no crack growth had occurred.

The results of this experiment suggest that a high flow velocity of water past the crack mouth prevents SCC initiation, but no information on the influence of flow velocity on crack propagation under high- and low-flow-rate conditions was obtained. Another test is planned in which SCC cracks will be initiated in both specimens under "quasi-static" low-flow conditions and then a high flow velocity will be imposed across the crack mouth of one of the specimens. The response of this specimen to alternate periods of high and low flow velocities will quantify the effect of this variable on crack propagation and establish whether periods of high flow velocity decrease the crack growth rate or significantly delay the onset of crack growth under subsequent low-flow conditions.

Development of Baseline Fracture Mechanics Crack Data

Fracture-mechanics crack-growth tests have been performed on two 0.7T compact tension specimens, one of CF3M cast SS (specimen No. CTC24-1) and the other of Type 316NG SS (Heat No. D440104, specimen No. 104-1). The ferrite level of the cast material was 5%, as determined by magnetic permeability measurements. The specimens were first precracked in high-temperature water with 0.2-0.3 ppm oxygen and 0.1 ppm sulfate at 289°C under a cyclic load (sinusoidal wave shape, 0.1 Hz) of R = 0.25. During the precracking, the specimens were inadvertently overloaded to a maximum stress intensity of 43 $MPa \cdot m^{1/2}$ for the CF3M SS and 38 $MPa \cdot m^{1/2}$ for Type 316NG SS. Crack growth testing was then attempted in the same environment under a cyclic load (sawtooth wave shape, 12-s rise and 1-s fall time) with R = 0.95 at a maximum stress intensity of 30 $MPa \cdot m^{1/2}$ for CF3M SS and 27 $MPa \cdot m^{1/2}$ for Type 316NG SS. No crack propagation was observed in either of the specimen for 740 h. The crack growth test was interrupted and the specimens were fatigue precracked again in the same environment under a cyclic load (sinusoidal wave shape, 0.1 Hz) of R = 0.4 at a lower maximum stress intensity of 25 $MPa \cdot m^{1/2}$. During 196 h of precracking, the cracks propagated 1.44 mm in the cast SS and 0.41 mm in the Type 316NG SS. This gives an average crack growth rate of 2×10^{-9} $m \cdot s^{-1}$ for the

cast SS specimen and 6 x 10^{-10} m·s^{-1} for the Type 316NG SS specimen. Crack lengths were measured by the d.c. electric potential and compliance measurement techniques. The measurements obtained by the two techniques were in good agreement. The values obtained for the cast SS specimen by the d.c. potential and the compliance techniques were 1.44 and 1.35 mm, respectively.

As a result of the crack growth, the maximum stress intensity values increased to 28 MPa·m$^{1/2}$ for the cast SS and 26 MPa·m$^{1/2}$ for the Type 316NG SS specimens. The crack growth test was resumed under a cyclic load of R = 0.95 at these maximum stress intensity values; however, the specimens were accidentally overloaded again and the test was terminated. The test will be resumed with a new set of 0.7T compact tension specimens prepared from the same heats of materials.

2.2.2 Constant Extension Rate Tests (P. S. Maiya)

CERT results for several heats of Type 316NG SS (see Table 2 for chemical compositions) reveal significant variations in susceptibility to SCC. Typical results are shown in Table 3. No simple correlation has been found between the resistance to crack growth and the minor variations in chemical composition among these heats.

It is known that susceptibility to TGSCC in chloride solutions decreases significantly as the concentration of nickel in the alloy increases.[7] However, the results in Table 3 indicate that TGSCC of the different heats of steel in the sulfate solution does not correlate with nickel content. Silicon, beryllium, and copper also appear to be "beneficial" insofar as resistance to chloride cracking is concerned.[7,8] The effect of silicon on SCC of low-carbon (<0.02 wt.%) austenitic stainless steels in boiling 42% $MgCl_2$ solution has been investigated by Hochman and Bourrat.[8] Their results suggested a consistent increase in resistance to cracking with increases in silicon content from 0.06 to 4.0 wt.%. Although the chloride and sulfate environments in the present tests are very different from the $MgCl_2$ environment, the results obtained from several heats show a similar trend. For example, in the experiments summarized in Table 4, the heat with the lowest silicon content (Heat No. 08076) is relatively susceptible and the heat with the highest silicon content (Heat No. 467958) is the most resistant. However, the Sumitomo heats, with approximately the same silicon content, still show a significant variation in TGSCC susceptibility, which suggests that other residual elements influence the SCC behavior.

Several heats of Type 316NG SS were analyzed to determine whether the origin of heat-to-heat variations can be attributed to the presence of trace elements such as P, S, Cu, V, Ti, and Pb. The results of the analyses are shown in Table 5. No correlation between cracking susceptibility and residual elements has been found.

CERT tests have also been performed on 5 different heats of Type 347 SS. The chemical compositions of these heats are shown in Table 6. Specimens from Heat Nos. 174100 and 170162 were tested in the welded condition in water containing 0.25 ppm dissolved oxygen and 0.1 ppm sulfate (added as acid) at strain rates between 10^{-6} and 10^{-7} s^{-1}. These results have been reported previously.[9] In these specimens, failure always occurred in the base metal outside of the heat-affected zone. As expected, an additional

Table 2. Chemical Compositions (wt.%) of Different Heats of Type 316NG SS

Element[a]	P91576	467958	08056	59076	NDE-28	Four Sumitomo Heats
C	0.015	0.02	0.02	0.018	0.014	0.012–0.019
Mn	1.63	1.51	1.55	1.44	1.77	1.66–1.75
P	0.02	0.029	0.022	0.022	0.02	0.011–0.018
S	0.01	0.008	0.0185	0.018	0.002	0.002–0.002
Si	0.42	0.635	0.295	0.60	0.52	0.45–0.49
Ni	10.95	12.74	11.00	12.83	13.58	12.85–13.35
Cr	16.42	17.14	16.37	17.41	17.79	17.29–17.91
Mo	2.14	2.43	2.09	2.48	2.59	2.3–2.59
Cr	–	0.16	0.33	0.48	0.11	0.05–0.12
N	0.068	0.069	0.075	0.0715	0.11	0.098–0.1
B	0.002	0.002	0.0005	0.0008	0.0006	0.005–0.008

[a]Balance is Fe for all heats.

Table 3. Heat-to-Heat Variations in SCC Susceptibility of Type 316NG SS[a]

Heat No.	t_f, h	ε_f, %	σ_{max}, MPa	$\dot{a}_{av}$, $m \cdot s^{-1}$
P91756	474.0	34.1	461	7.35×10^{-10}
467958	577.0	41.6	501	0
08056	641.0	46.0	390	4.38×10^{-10}
59076	398.1	28.7	487	3.83×10^{-10}
NDE-28	653.0	47.0	470	1.28×10^{-9}
D440104	712.0	51.0	464	3.49×10^{-10}
D472701	647.0	46.6	455	2.97×10^{-10}
D442604	669.0	48.2	463	0
D450905	664.0	47.8	468	7.41×10^{-11}

[a]All specimens were heat treated for 1050°C/0.5 h + 650°C/24 h. Tests were conducted in water with 0.25 ppm dissolved oxygen and 0.1 ppm sulfate, at 289°C and a strain rate of $2 \times 10^{-7}\ s^{-1}$.

Table 4. Effect of Si Content on Crack Growth Rate of Type 316NG SS[a]

Heat No.	Si, wt.%	$\dot{\epsilon}$, s^{-1}	Oxygen and Impurity Content in Water, ppm	$\dot{a}_{av}$, $m \cdot s^{-1}$
08076	0.295	2×10^{-6}	$8\ O_2 + 0.5\ Cl^-$	3.74×10^{-9}
		2×10^{-7}	$0.25\ O_2 + .1\ SO_4^{2-}$	4.38×10^{-10}
P91756	0.42	2×10^{-6}	$8\ O_2 + 0.5\ Cl^-$	2.30×10^{-9}
		2×10^{-7}	$0.25\ O_2 + 1\ SO_4^{2-}$	7.35×10^{-10}
467958	0.635	2×10^{-6}	$8\ O_2 + 0.5\ Cl^-$	0
		2×10^{-7}	$0.25\ O_2 + 1\ SO_4^{2-}$	0

[a]CERT specimens were heat treated for 1050°C/0.5 h + 650°C/24 h prior to tests. All tests were performed at 289°C.

Table 5. Trace Element Analysis (wt.%) for Type 316NG SS

Heat No.	P	S	Pb	Cu	V	B	Ti
P91756	0.016	0.011	0.002	0.19	0.05	0.0035	0.01
467958	0.024	0.006	0.002	0.16	0.04	0.0032	<0.01
08056	0.021	0.022	0.002	0.34	0.07	0.0008	<0.01
59076	0.015	0.02	0.002	0.43	0.08	0.002	0.03
NDE-28	0.013	0.002	0.002	0.10	0.02	0.0008	<0.01
D440104	0.015	0.002	0.003	0.11	0.05	0.0006	<0.01
D472701	0.02	0.003	0.002	0.07	0.04	0.0008	<0.01
D442604	0.016	0.002	0.002	0.06	0.06	0.0009	0.01
D450905	0.014	0.004	0.002	0.05	0.04	0.0009	0.01

[a]Zr, Zn, and Al are present at levels of <0.01 wt.%.

Table 6. Chemical Compositions (wt.%) of Different Heats of Type 347 SS

Element[a]	174100	170162	869962	LPN	316642	30316[b]
C	0.03	0.03	0.04	0.019	0.03	0.017
Mn	1.7	1.7	1.56	1.581	1.56	1.61
P	0.036	0.012	0.017	0.014	0.023	0.018
S	0.015	0.019	0.0020	0.005	0.014	0.002
Si	0.33	0.43	0.46	0.23	0.29	0.8
Ni	11.0	10.75	9.69	9.28	10.81	10.85
Cr	18.15	18.53	18.34	18.68	18.06	19.53
Mo	0.48	0.35	0.18	0.01	0.29	0.03
Cu	0.12	0.11	0.05	0.01	0.09	0.04
N	0.029	0.0212	0.0193	0.069	0.021	–
B	0.005	0.0005	0.002	0.001	0.0009	–
Nb	0.44	0.51	0.60	0.25	0.60	0.61

[a] Balance is Fe for all heats.
[b] Filler material.

500°C/24 h heat treatment had no effect on susceptibility to TGSCC.

Specimens from three additional heats (Heat Nos. 869962, LPN, and 316642) were tested under similar environmental and loading conditions. The CERT specimens were solution-annealed at 1050°C for 0.5 h and quenched, and then heat treated at 650°C for 24 h. The CERT results for these materials, along with the previously reported results on the other heats, are summarized in Table 7. Except for Heat No. 316642, all the heats of material were susceptible to TGSCC. However, susceptibility was observed only at strain rates of $<5 \times 10^{-7}$ s^{-1}, which are lower than those generally required to induce TGSCC in Type 316NG SS in these environments.

The strain rate at or below which SCC occurs is the (upper bound) critical strain rate. Above this critical strain rate, purely mechanical failure dominates. In this regime, there is a linear relationship between the time to failure and the applied strain rate corresponding to the mechanical failure. For applied strain rates less than the critical strain rate, the relationship between the time to failure and the applied strain rate is nonlinear (i.e., the slope is less than one on a log-log plot of the time to failure versus the applied strain rate). This upper-bound critical strain rate depends on the material and the environment. The lower the critical strain rate, the more resistant the material is to SCC.

The critical strain rates for sensitized Types 304 and 316 SS and 316NG (nonsensitized) SS are identified in Fig. 4. In terms of the critical strain rate, Type 316NG SS is more resistant to SCC than sensitized Types 304 and 316 SS. Type 347 SS is somewhat superior to Type 316NG SS in terms of this measure of resistance to SCC.

As the results in Table 7 indicate, Heat No. 316642 of Type 347 SS is extremely resistant to SCC in the sulfate solution after heat treatment at 1050°C/0.5 h followed by 650°C/24 h. To determine whether different heat treatments or different thermomechanical histories have an effect on TGSCC susceptibility, CERT specimens from this heat were also prepared from welded plate. These specimens (designated as K2W—X) were fabricated such that the weld interface was located

Table 7. Heat-to-Heat Variations in SCC Susceptibility of Type 347 SS

Test No.	Heat No.	$\dot{\epsilon}$, s^{-1}	t_f, h	σ_{max}, MPa	Failure	$\dot{a}_{av}$, $m \cdot s^{-1}$	SS Potential, mV(SHE)
263	174100	1×10^{-6}	65.5	432	Ductile	0	21
274	174100	5×10^{-7}	114.5	417	TGSCC	1.63×10^{-9}	94
272	174100	2×10^{-7}	301.5	448	TGSCC	1.10×10^{-9}	-8
275	174100	1×10^{-7}	574.5	451	TGSCC	7.58×10^{-10}	55
301	170162	1×10^{-6}	55.7	427	Ductile	0	84
305	170162	5×10^{-7}	114.1	430	Ductile	0	91
310	170162	2×10^{-7}	250.5	471	TGSCC	5.50×10^{-10}	22
349	869962	1×10^{-6}	94.5	460	Ductile	0	22
350	869962	5×10^{-7}	182.8	466	TGSCC	3.80×10^{-10}	34
348	869962	2×10^{-7}	442.0	472	TGSCC	2.97×10^{-10}	80
364	316642	1×10^{-6}	100.0	438	Ductile	0	-1
365	316642	5×10^{-7}	198.0	444	Ductile	0	3
367	316642	2×10^{-7}	487.0	443	Ductile	0	-87
382	LPN	1×10^{-6}	93.8	452	Ductile	0	86
380	LPN	5×10^{-7}	174.8	459	TGSCC	1.22×10^{-9}	90
377	LPN	2×10^{-7}	530.5	460	TGSCC	9.83×10^{-10}	-54

[a]All tests were performed in water with 0.25 ppm dissolved oxygen and 0.1 ppm sulfate at 289°C.

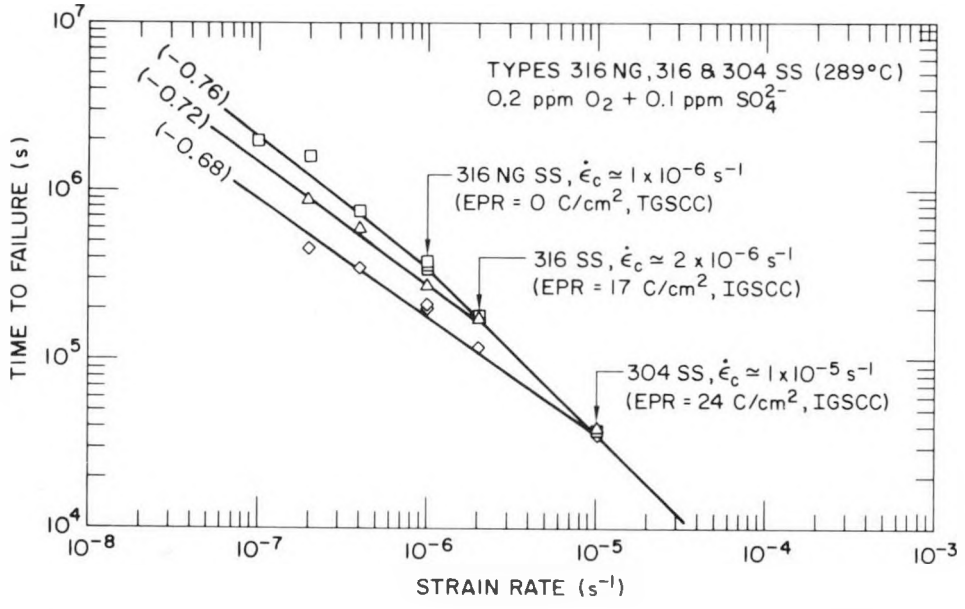

Figure 4. Time To Failure as a Function of Applied Strain Rate, Showing the Upper Bound Critical Strain Rate for SCC.

approximately in the center of the gage section (as in the welded specimens from Heat Nos. 174100 and 170162), and tested at the same strain rates as those used for the base metal. The specimens were tested both in the as-welded condition and after a subsequent 500°C/24-h heat treatment. The results of these tests are given in Table 8 along with results for the base metal specimens (designated as K2--X). No cracking is observed in the weld specimens at strain rates of either 1×10^{-6} or 5×10^{-7} s^{-1}, although the strains to failure are lower by approximately 50% for the weldments, as expected. However, at a strain rate of 2×10^{-7} s^{-1}, cracking occurred in the weld specimen but not in the base metal specimen. The crack was located in the base metal relatively far from the weld. Although a very low critical strain rate was observed for this material, the average crack growth rate for specimen no. K2W-3 is greater than the crack growth rate observed for specimens from other heats of Type 347 SS (Heat Nos. 174100, 170162, and 869962) by a factor of ~2-8.

Additional tests were performed on material from Heat No. 316642 in the solution-annealed condition (1050°C/0.5 h, water quenched) at strain rates of 2×10^{-7} and 1×10^{-7} s^{-1}. The results of these tests are summarized in Table 8. The material, which is extremely resistant to TGSCC in the aged condition, becomes susceptible to TGSCC in the solution-annealed condition. Although heat treatment at 650°C/24 h appears to increase resistance to cracking, a specimen with a heat treatment of 600°C/24 h cracked at about the same rate as the solution-annealed material. Similarly, the crack growth rates for the specimens in the as-welded condition are not significantly affected by an additional 500°C/24-h heat treatment.

To better understand the possible effects of heat treatment on susceptibility to SCC, specimens from three heats of Type 347 SS (Heat Nos. 174100, 170162, and 869962) were metallographically prepared and electrolytically etched with 10% oxalic acid, and the precipitate size and morphology were examined by SEM. All the heat-treated specimens contain precipitates (Fig. 5), which were Nb-rich as determined by energy-dispersive x-ray analysis (Fig. 6). The precipitates are less than a micrometer in diameter. As is shown in Fig. 5, the crack growth rates appear to decrease with an increase in precipitate size.

The increased resistance to crack growth with an increase in precipitate size is consistent with the idea that precipitates offer resistance to slip and hence can retard the film rupture process that is generally involved in the crack growth process. Qualitatively, alloys in which dislocation movement is coplanar are the most susceptible to TGSCC in boiling $MgCl_2$ solution.[10] The relative character of the slip process (planar versus cross slip) depends on the nature of the alloying elements and the presence or absence of a precipitate structure. The relationship between some of the alloying elements and stacking fault energy (SFE), as determined by Douglass et al.,[10] is shown in Fig. 7. The general trend shows that SFE increases with nickel content. This is consistent with observations that SCC susceptibility decreases with an increase in nickel content. The results also show that the presence of Nb (or Ti) in solid solution markedly decreases SFE; this effect should increase susceptibility to TGSCC as a result of the increased slip planarity. Our CERT results on solution-annealed Type 347 SS are at least qualitatively consistent with the above mechanistic ideas.

Table 8. Effect of Heat Treatment on SCC Susceptibility of Type 347 SS[a]

Test No.	Specimen No.	$\dot{\varepsilon}$, s^{-1}	t_f, h	ε_f, %	ε_u, %	σ_{max}, MPa	$\Delta A/A_o$, %	SS Potential, mV(SHE)	$\dot{a}_{av}$, $m \cdot s^{-1}$
			Heat treatment: 1050°C/0.5 h + 650°C/24 h (air cooled)						
364	K2-1[b]	1×10^{-6}	100	36.0	28.8	438	59	-1	0
365	K2-2	5×10^{-7}	198	35.6	30.1	444	63	3	0
367	K2-3	2×10^{-7}	487	35.1	28.8	443	55	-87	0
			Heat treatment: 1050°C/0.5 h + 600°C/24 h						
408	K2-7	2×10^{-7}	320.0	23.0	20.4	435	16	119	1.37×10^{-9}
			Heat treatment: 1050°C/0.5 h (water quenched)						
399	K2-6	2×10^{-7}	478.5	34.5	32.0	444	45	45	1.27×10^{-9}
398	K2-5	1×10^{-7}	923.0	33.2	30.5	446	22	83	9.30×10^{-10}
			Heat treatment: As welded + 500°C/24 h						
387	K2W-2[c]	1×10^{-6}	50.5	18.2	11.5	445	54	88	0
385	K2W-1	5×10^{-7}	126.9	22.8	17.3	455	54	100	0
389	K2W-3	2×10^{-7}	184.0	13.2	10.4	455	46	68	2.26×10^{-9}
396	K2W-4	2×10^{-7}	210.0	15.1	13.2	454	21	29	1.92×10^{-9}
			Heat treatment: As welded						
397	K2W-5	2×10^{-7}	307.0	22.1	19.1	456	39	110	1.72×10^{-9}

[a]All tests were performed in water with 0.25 ppm dissolved oxygen and 0.1 ppm sulfate at 289°C.
[b]Specimens numbered K2-X: base metal.
[c]Specimens numbered K2W-X: weldment.

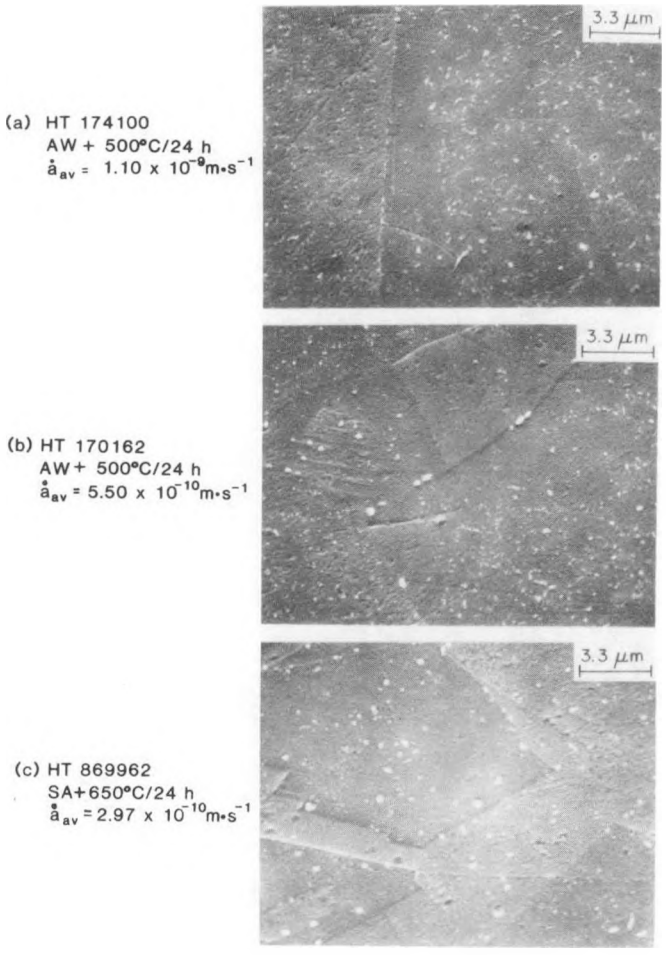

Figure 5.
Precipitate Distributions in Type 347 SS and Corresponding Crack Growth Rates.

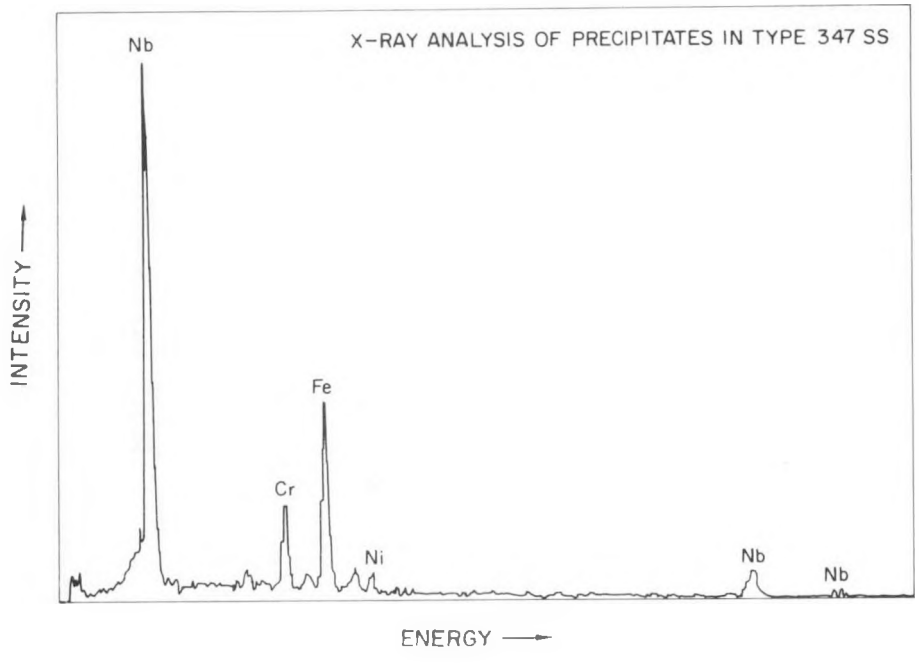

Figure 6. X-Ray Analysis of a Typical Precipitate Observed in Heat No. 869962.

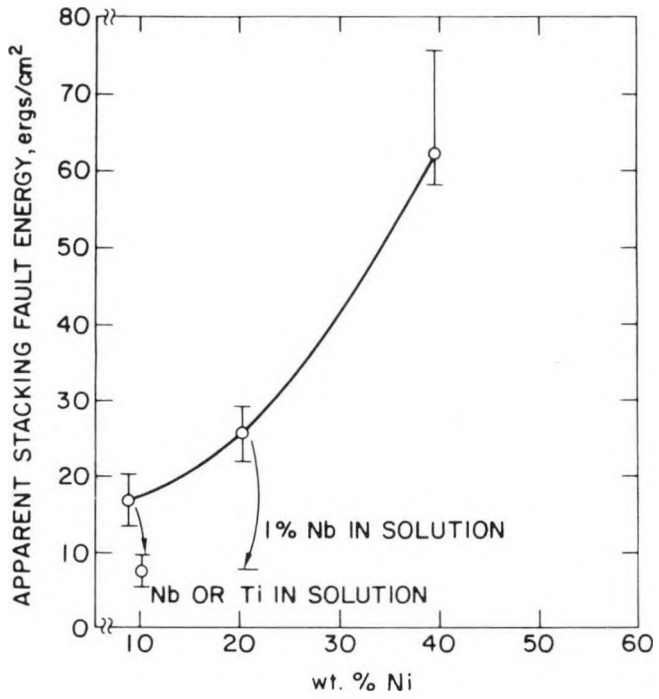

Figure 7. Effect of Nickel on Apparent Stacking Fault Energies of Austenitic Alloys Containing 20 wt.% Cr (Adapted from Reference 10). Arrows indicate lowering of stacking fault energy by Nb in solid solution resulting from solution-annealing heat treatment.

2.2.3
Fatigue of Type 316NG Stainless Steel (W. J. Shack and W. F. Burke)

Residual-life assessment reviews for LWRs indicate that low-cycle fatigue is a potentially significant degradation mechanism in LWR primary piping, which must be considered to justify extended operation of the plant.[11] Current fatigue design for this piping is based on the ASME Section III Fatigue Design Curves.[12] Environmental effects are not explicitly considered in these curves. Instead, the design curves are obtained by introducing a factor of 2 on the strain range or 20 on the cycles from the mean life curve, whichever is more conservative. Studies by General Electric under EPRI sponsorship[13] show that the effect of the standard BWR environment on the fatigue life of A106-GrB and A333-Gr6 can completely erode the "2 or 20" margin in the Code Design Curve, as shown in Fig. 8. Other work has shown that the design margin for low-alloy A-516 steel also decreased significantly in BWR environments.[14] However, ongoing work under USNRC sponsorship has shown that PWR environments appear to have much less effect on cyclic crack growth in A106-GrB material than BWR environments.[15]

Environmental effects on the fatigue life of Types 304 and 304L SS were investigated in the Dresden I reactor with bend specimens rather than conventional uniaxial specimens.[14] Even though the plastic strain ranges in these tests were fairly high (0.5, 0.75, and 1.0%), the BWR environment had a significant effect on sensitized materials under both fully reversed loading (equal compression and tension) and zero-tension loading in these tests. As shown in Fig. 9, the environment significantly affected the as-received materials only under zero-tension loading. It is possible that environmental degradation would be even more significant at lower strain ranges.

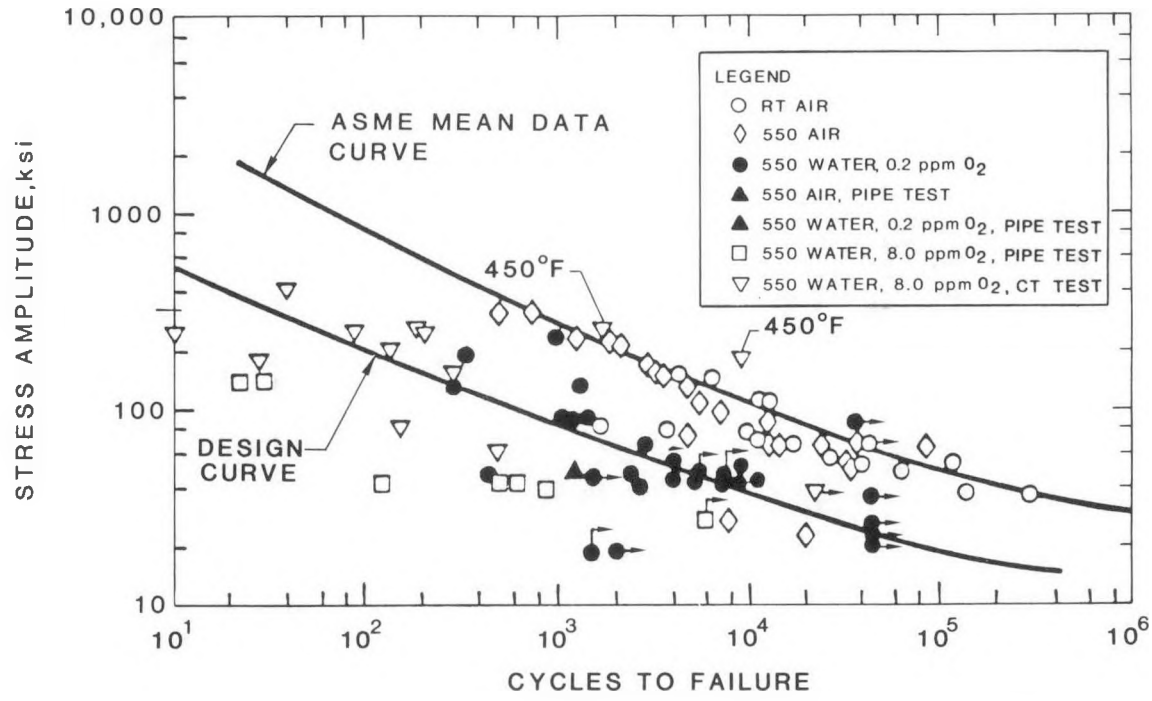

Figure 8. Comparison of Fatigue Test Results for Carbon Steel Fatigue Specimens and Pipe Test Specimens at 288°C (550°F) with the ASME Section III Design and Mean Data Curves (Adapted from Reference 13).

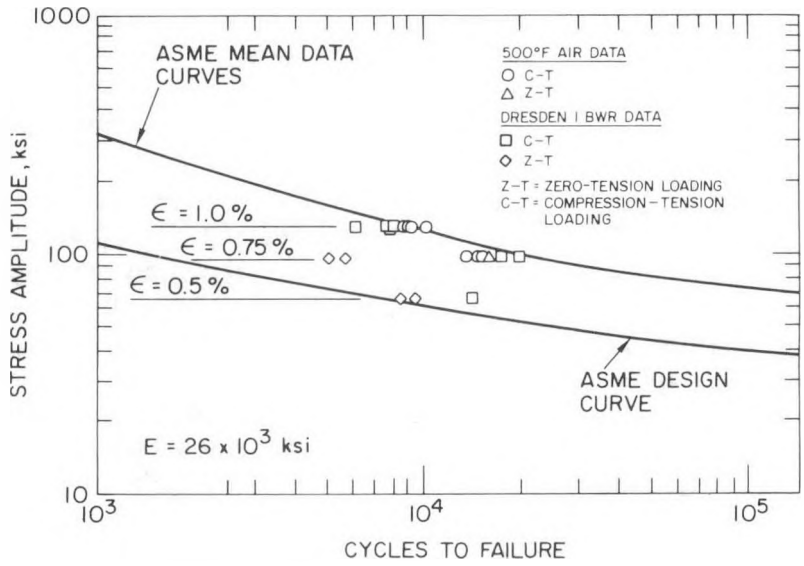

Figure 9. Comparison of Fatigue Test Results on As-received Type 304 SS in the Dresden I Reactor with the ASME Section III Design and Mean Data Curves (Adapted from Reference 14).

A limited number of tests were performed to evaluate the fatigue behavior of Type 316NG SS in work sponsored by the BWR Owners Group to developed alternative alloys for BWR piping systems.[16] Although all the data were above the ASME Section III Design Curve, as shown in Fig. 10, it appears that the environment eliminated a substantial portion of the safety margins built into the Code.

The objective of the current work is to provide additional information on the effects of operating temperature and environment on the fatigue behavior of Type 316NG SS. The data obtained will be used to assess the degree of conservatism inherent in the ASME Code Section III Fatigue Design Curves for this material. It may also be needed for decisions on life extension beyond the current 40-year design life.

The material for the test program is Type 316NG SS from 22-in.-diam pipe manufactured by Sumitomo. It is actually a stub from the new recirculation piping system installed at the Cooper BWR. The specimens are fabricated from the piping material with no additional heat treatment so that the condition of the material is as close as possible to the actual piping material.

The fatigue tests will be performed in autoclaves of the type that have been used for our CERT tests. Schematics of the autoclave system and the specimen design are shown in Figs. 11 and 12, respectively. The fatigue specimens are much longer than the CERT specimens so that the connections to the load frame can be made outside the autoclave. This eliminates the need for threaded connections, which make specimen alignment difficult. The tests will be performed in MTS servohydraulic load frames with MTS hydraulically actuated grips.

Baseline in-air tests are being performed with the same specimen design and loading systems that will be used for the tests in the LWR environment. Prior to the start of the fatigue tests, preliminary studies were performed on specimens instrumented with strain gages to ensure that excessive bending strains would not occur. Two 0.375-in.-diam specimens, one with a center gage section of 0.750 in. and one with a center gage section of 0.937 in., were instrumented and tested to determine the bending strains as a function of the axial strain range. The tests were performed in stroke control. The specimens were loaded to a given stroke value and cycled. Strain gage readings were made at the peak tensile and compressive stroke positions after one cycle and then repeated after an additional ten cycles. At a few levels, readings were repeated after additional cycles, but the number of cycles was restricted to avoid fatigue of the cement bonds between the gages and the specimens. The results for the two specimen types are summarized in Table 9. The relative bending, i.e., the maximum bending strain divided by the axial strain range, in the 0.937-in. gage-length specimen is satisfactory (<0.03) for axial strains up to ~0.75%. The relative bending in the 0.750-in. gage-length specimen was satisfactory over the entire strain range investigated (0–1.6%); the test was terminated because of a failure of a bond between one of the gages and the specimen. The 0.750-in. gage-length specimen design will be satisfactory over the strain range of possible interest and was selected for the fatigue test program.

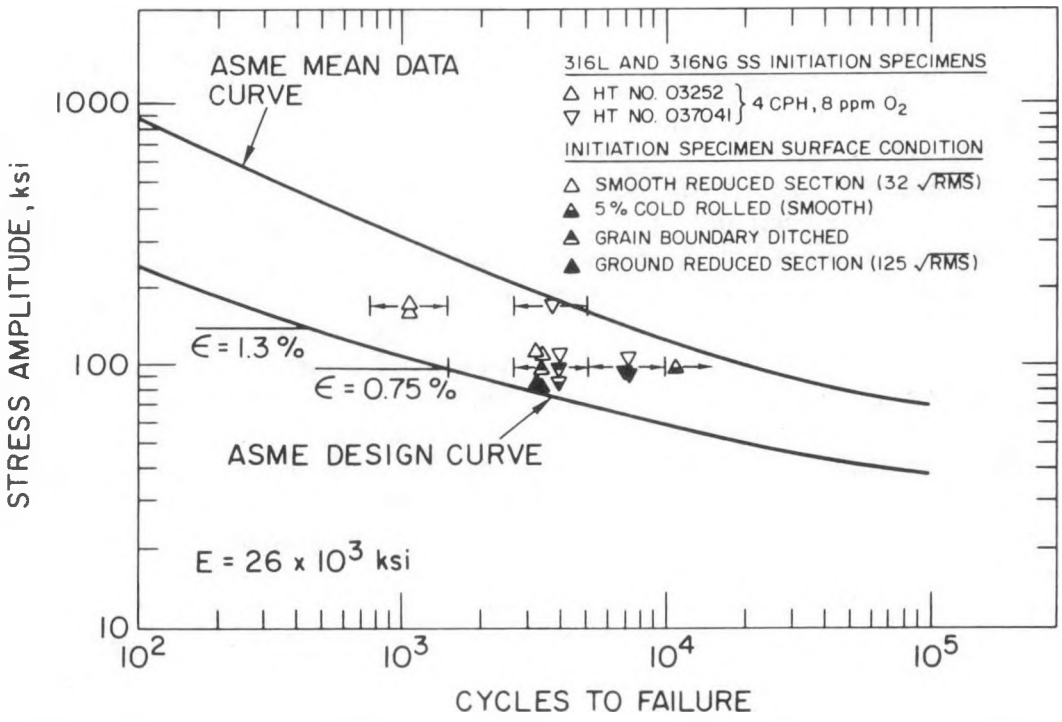

Figure 10. Comparison of Fatigue Test Results on Type 316NG SS in Simulated BWR Environments with the ASME Section III Design and Mean Data Curves (Adapted from Reference 16).

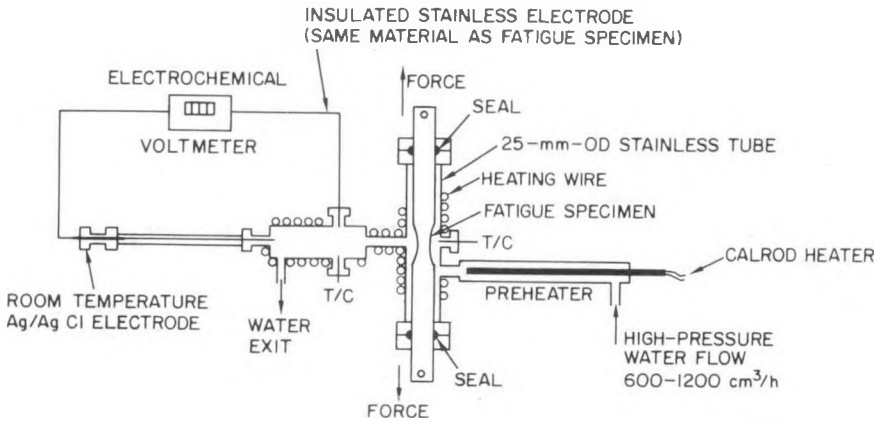

Figure 11. Schematic of Autoclave Test System for Fatigue Tests in LWR Environments.

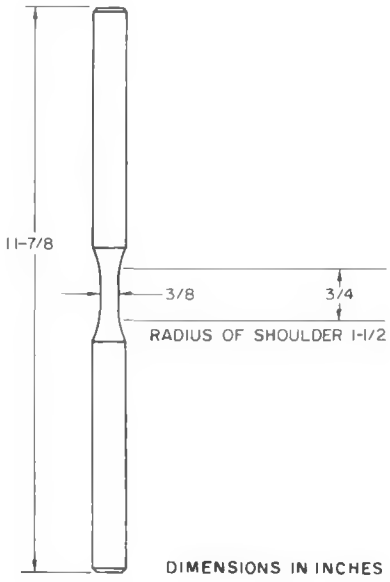

Figure 12.
Fatigue Test Specimen.

Table 9. Relative Bending (Maximum Bending Strain/Axial Strain Range) in Specimens with Two Different Gage Lengths

Stroke (mils)	Strain range (%)	Relative Bending
	0.750-in. Gage Length	
0.63	0.036	0.006
1.5	0.088	0.003
3.0	0.179	0.007
6.0	0.606	0.026
7.0	0.763	0.019
8.0	0.913	0.016
9.0	1.051	0.015
10.0	1.188	0.013
11.0	1.322	0.016
12.0	1.476	0.021
13.0	1.644	0.022
	0.9375-in. Gage Length	
[a]	0.037	0.011
1.5	0.087	0.011
3.0	0.177	0.011
4.5	0.330	0.033
6.0	0.546	0.011
7.0	0.672	0.012
8.0	0.822	0.029
9.0	0.943	0.041
10.0	1.100	0.061

[a]No stroke measurement was recorded for this strain range.

Baseline tests in air at room temperature (~22°C) have been completed. The results of these tests are summarized in Table 10. Figure 13 compares these results with the design curve for austenitic stainless steels in ASME Section III and with the ASME mean data curve.[17] The results are in good agreement with the mean data curve for fairly short lives corresponding to plastic strain ranges of greater than 0.5%, but they fall below the mean data curve at longer lives. This does not necessarily indicate that the fatigue strength of the Type 316NG SS is less than that of Type 304 SS. The mean data curve is based almost entirely on tests with lives of less than 10^5 cycles.[17] The mean data curve at lower linear stress amplitudes was obtained by extrapolation of the available data. The results for Type 316NG SS are close to the actual data for Type 304 SS. The departure from the mean data curve occurs only for the portion of the curve that is extrapolated beyond the range of the supporting data base.

2.2.4 Effect of Surface Cold Work on Crack Initiation in Alternative Alloys (J. Y. Park)

Crevice bent-beam SCC tests on Type 316NG SS (Heat No. P91576 plate and Heat No. NDE-28 pipe) are continuing in high-purity water with 0.2-0.3 ppm dissolved oxygen at 289°C. The specimens from Heat No. P91576 were fabricated from 1-in.-thick plate and shot peened to three different levels. Some of these specimens were furnace heat treated for 24 h at 500 or 600°C after the shot peening. The specimens from Heat No. NDE-28 were fabricated from the inside

Table 10. Cycles to Failure as a Function of Strain Range for Room Temperature Strain-controlled Fatigue Tests on Type 316NG SS

Test Number	Strain Range, %	Cycles to Failure
1390	0.75	25,736
1391	1.0	13,561
1392	0.5	60,741
1393	0.4	127,386
1394	1.5	4,649
1395	0.35	183,979
1396	0.75	30,000
1397	0.30	347,991
1398	0.27	~666,000
1399	0.25	[a]
1400	0.25	~1,775,000

[a]Test 1399 failed at ~1,900,000 cycles because of an equipment malfunction.

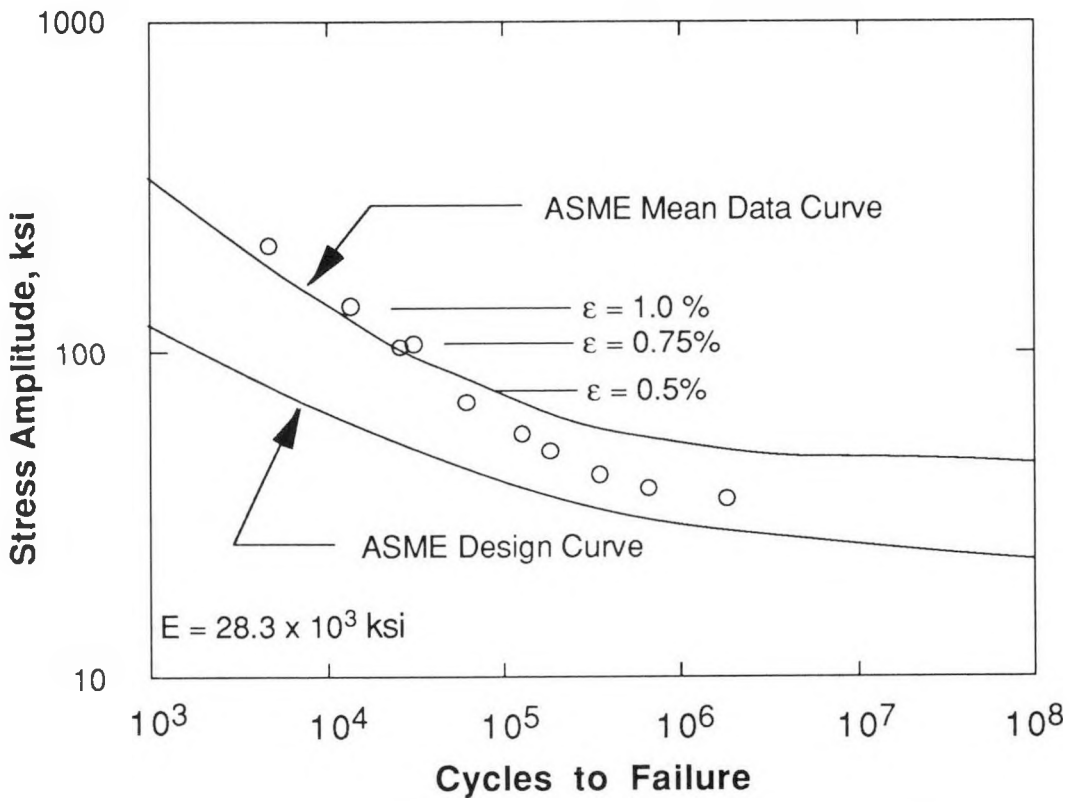

Figure 13. Comparison of Current Results on Fatigue of Type 316NG SS at Room Temperature in Air with the ASME Section III Design and Mean Data Curves.

diameter of the pipe near the weld heat-affected zone. Specimens and specimen holders (Fig. 14) are designed to provide a 0 to 0.25-mm crevice and 15% total strain. The accumulated test time has reached 3000 h. The tests will be interrupted at an accumulated test time of 5000 h and the specimens will be examined for evidence of SCC.

3 Influence of Water Chemistry on SCC of Type 304 SS

3.1 Introduction

The objective of this work is to evaluate the potential effectiveness of proposed actions to solve or mitigate the problem of IGSCC in BWR systems through modifications of water chemistry. In this regard, the effects of dissolved oxygen (produced by radiolytic decomposition of the water), anion impurities (e.g., oxyacids from decomposition of ion exchange resins during intrusions into the primary system), and several corrosion-product cations on the IGSCC susceptibility and crack growth properties of austenitic stainless steels have been evaluated. The potential benefits associated with small additions of hydrogen to the coolant were also evaluated under conditions in which ionic impurities (viz., oxyanions) were also present at low concentrations in the high-temperature water.

The results of this work suggest that SCC of the sensitized steel is controlled by the rate of cathodic reduction of dissolved oxygen, various oxyanion impurity species,

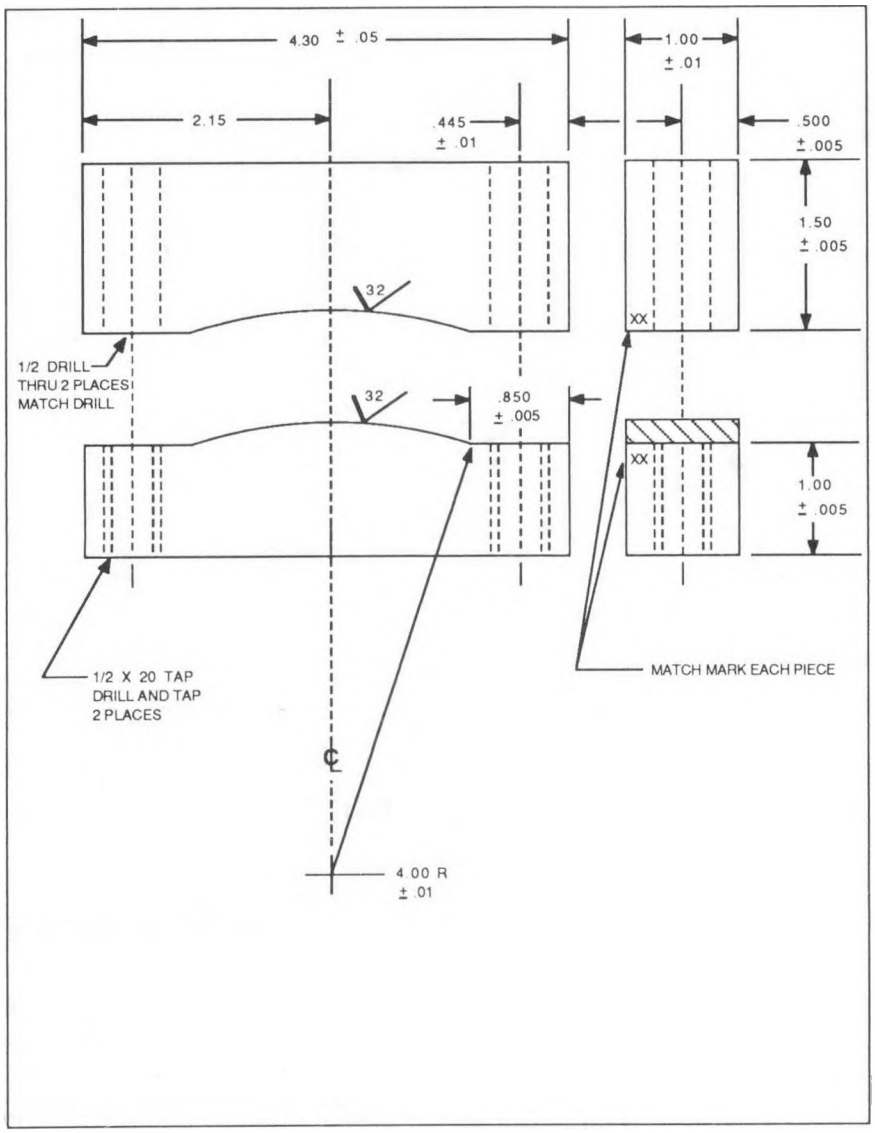

Figure 14. Crevice Bent-Beam Test Fixture. Dimensions in inches.

and Cu^{2+} in the high-temperature water.[18-21] The crack growth behavior of the steels was correlated with the type and concentration of impurities in the water as well as the open-circuit corrosion potential of the steel.

3.2 Technical Progress

3.2.1 Effect of Dissolved Copper on SCC (W. E. Ruther, W. K. Soppet, and T. F. Kassner)

Metallic impurities (viz., corrosion products) from the feedwater train are transported in the reactor water along with various ionic species that can enter BWR

coolant water from leaks in condenser tubes and from the condensate polishing system itself, including resin fines. In addition to soluble and insoluble iron, copper is also present in the water in plants with admiralty brass, aluminum brass, or copper-nickel condenser tubes and/or copper alloy feedwater heaters. The copper concentration in BWR water is of primary concern from the standpoint of deposition on the Zircaloy fuel cladding, which can lead to crud-induced localized corrosion (CILC) and fuel element failures at relatively low burnup.[22,23] The CILC failures occurred primarily in $(U,Gd)O_2$ fuel rods in BWRs with admiralty brass condensers and filter-demineralizer condensate water cleanup systems, which are not as effective as deep resin beds for removal of copper from the water.[23]

Copper corrosion products are also present in secondary-system water of pressurized water reactors (PWRs) and can lead to pitting of steam generator tubes[24,25] and contribute to accelerated corrosion of carbon steel tube support plates.[26,27] The effect of copper species at low concentrations on the SCC of reactor materials has not been studied as extensively as that of other impurity species; however, cupric ion at relatively high concentrations in oxygenated[28] (200 ppb) and deoxygenated[20,21] (<5 ppb) high-temperature water promotes IGSCC of sensitized Type 304 SS. Cupric and cuprous ion, in contrast to other cations (viz., Zn^{2+}, Mg^{2+}, and Na^{+}) that have a single oxidation state, can contribute to SCC by providing a cathodic-reduction partial process that couples with the anodic dissolution at the crack tip in a slip-dissolution mechanism[29,30] for crack growth.

During this reporting period, the effect of cuprous chloride on the SCC susceptibility of sensitized Type 304 SS was investigated at several temperatures between 135 and 289°C. The CERT experiments were performed in low-oxygen (<5 ppb), near-neutral water to minimize the contribution of other species that can also undergo cathodic reduction (viz., O_2 and H_3O^{+}). The role of pH in SCC susceptibility of the steel, for several copper concentrations in the feedwater, is also being investigated at 200°C. The effect of several organic ethylenediaminetetra-acetate (EDTA) salts, in feedwater containing 0.2 ppm dissolved oxygen, on the SCC characteristics of the steel was determined at 289°C.

Effect of Temperature and Cu^{+} Concentration

Previous CERT results[20,21] indicated that the minimum Cu^{2+} concentration required for severe IGSCC of the steel was a function of temperature (e.g., ~1 ppm Cu^{2+} at 289°C and ~0.1 ppm at 150°C). These values are considerably higher than those encountered in the feedwater of BWRs (<0.3 ppb)[31] or in secondary-system water in recirculating and once-through steam generators of PWRs (<2 ppb).[32] In BWRs with feedwater heaters and/or a condenser fabricated from copper-base alloys, the reactor coolant water typically contains <35 ppb of copper.[33,34] Consequently, Cu^{2+} at low concentrations in the water would not be expected to contribute to SCC of steel in high-temperature regions of the reactor coolant circuit. However, potential-pH (Pourbaix) diagrams for the $Cu-H_2O$ and $Fe-Cu-H_2O$ systems[34] indicate that the stability regime for Cu^{+} increases at the expense of Cu^{2+} as the temperature increases. Consequently, Cu^{+} and Cu° are the copper species most likely to be present under the potential-pH conditions found in both BWRs and PWRs.

A series of CERT experiments was performed to determine the minimum concentrations of Cu^{+} in low-oxygen water

for SCC of sensitized Type 304 SS at temperatures between 135 and 289°C. As in the previous tests, the presence of other species that can also participate in cathodic–reduction partial processes was minimized by adding Cu^+ to the feedwater as CuCl, which is only slightly soluble at 25°C. As in previous work, the open–circuit corrosion potential (ECP) of Type 304 SS and the redox potentials of platinum and copper were determined versus an external 0.1M KCl/AgCl/Ag reference electrode and the values were converted to the standard hydrogen electrode. The effluent water was collected, and the copper concentrations were determined by inductively–coupled–plasma (ICP) spectro–photometry analyses.

The feedwater chemistries, CERT parameters, and ECP results are given in Table 11. As in the case of the SCC data for this material in water containing $CuCl_2$, the failure mode of the specimens exhibits an abrupt transition from predominantly ductile fracture to IGSCC over a narrow Cu^+ concentration range at both 150 and 289°C (see Fig. 15). At 200°C, the crack growth rate of the steel increased with Cu^+ concentration in the feedwater, as shown in Fig. 16. The data are consistent with a line of slope ~1, which is consistent with a cathodic–reduction partial process of $Cu^+ + e^- = Cu°$ on the basis of the mass action relationship for this reaction and the heuristic relation according to which the crack growth rate is proportional to $1/[e^-]$ when the process is controlled by the rate of cathodic reduction of molecular species (e.g., O_2) or ionic species (SO_4^{2-}, NO_3^-, etc.) in the water.[18,19] Previous results at 150°C indicated an increase in the crack growth rate with the 1/2 power of the Cu^{2+} concentration over the range of ~0.1 to 10 ppm, which is consistent with a two–electron process during the reduction of Cu^{2+} to Cu°.[21]

The temperature dependence of the crack growth rate of the steel in low–oxygen water (<5 ppb) containing ~1–2 ppm Cu^+, a concentration at which IGSCC occurred at all temperatures between 135 and 289°C, is shown in Fig. 17. The broad maximum in the crack growth rate between ~170 and 250°C and the decrease in IGSCC susceptibility at both lower and higher temperatures are similar to features of the SCC behavior of the material in high–purity water containing 0.2 ppm dissolved oxygen and in water with 0.1 and 1.0 ppm sulfate at this oxygen concentration.[36,37] The crack growth rate of the steel at ~200°C in water with ~1–2 ppm Cu^+ is higher by factors of 10 and 3 than in high–purity water with 0.2 ppm dissolved oxygen and in similarly oxygenated water with 1 ppm sulfate, respectively.

The temperature dependence of the ECP of Type 304 SS, platinum, and copper (Fig. 18) is also similar to that obtained in low–oxygen water containing ~1–2 ppm Cu^{2+} and in oxygenated water with and without sulfate at low concentrations.[21] The effect of Cu^+ concentration in water containing <5 ppb dissolved oxygen on the ECP of Type 304 SS, platinum, and copper at several temperatures is shown in Figs. 19–21, respectively. The ECP values are plotted versus both the Cu^+ concentration and the conductivity of the feedwater. The data points in low–oxygen, high–purity water were obtained in the same facility as the CERT data, and by analogous methods; however, a CERT specimen was not strained during the time period in which the steady–state ECP values were determined at the three temperatures. The results indicate that ECP values of the three materials increase as the Cu^+ concentration or conductivity of the feedwater increases. At 289°C, IGSCC occurred at Type 304 SS ECP values of greater than –300 mV(SHE), as

observed when Cu^{2+} was added to the feedwater.[20] This value is consistent with a range of ECP values of approximately -200 to -300 mV(SHE), above which IGSCC occurs when other impurity ions are present in low-oxygen water at this temperature.[18,38] At 150 and 200°C, the scatter in the ECP values for Type 304 SS is somewhat greater than for the other materials. In contrast to Type 304 SS or copper, the ECP values of the platinum electrode (Fig. 20a) vary over a wide range [-400 to +300 mV(SHE)] as the Cu^{+} concentration of the water increases from ~0 to 2 ppm at 150 and 200°C.

Effect of pH in Several Cu^{+} Solutions at 200°C

The effect of pH on the SCC behavior of sensitized Type 304 SS is being investigated at 200°C in low-oxygen (<5 ppb) water containing 0.1 and 1.0 ppm Cu^{+} added as CuCl. The feedwater is altered by HCl or NH_4OH additions to produce pH values in the range of 3.6 to 8.7 at room temperature. For comparison with the results in the acid-chloride solutions containing Cu^{+}, CERT tests are also being conducted in the deoxygenated water containing HCl at low concentrations corresponding to $pH_{25°C}$ values between 3.6 and 5.7. Copper concentrations in the effluent water are being determined by ICP analyses.

The data reveal the following trends. At a constant $pH_{25°C}$ of ~4.7 (e.g., ~1.0 ppm HCl), the crack growth rates of the steel in water containing 0.1 and 1.0 ppm Cu^{+} were larger by factors of ~7 and 45, respectively, compared to that in water without cuprous ion. In deoxygenated water containing 0.5 to 10 ppm HCl ($pH_{25°C}$ of 5.0 to 3.6), the crack growth rate was relatively low, i.e., $2.5 \pm 0.4 \times 10^{-9}$ m·s^{-1} at a strain rate of 1×10^{-6} s^{-1}. At a $pH_{25°C}$ of <4.8, the effluent copper concentrations were higher than the concentration in the feedwater because of the dissolution of copper that deposited in the piping and heat exchanger of the CERT system during this series of experiments. At a $pH_{25°C}$ of 3.6 (10 ppm HCl) and an effluent copper concentration of ~6 ppm, the crack growth rate of steel was also larger by a factor of 45 compared with water containing 10 ppm HCl. In a basic solution containing 0.1 ppm Cu^{+} and NH_4OH ($pH_{25°C}$ = 8.7), the effluent copper concentration was lower by a factor of 10 than in the feedwater and no SCC occurred.

On the basis of these results and similar, previously reported[21] information obtained in water containing Cu^{2+}, cuprous and cupric ions at concentrations of >0.1 ppm in high-temperature, low-oxygen water strongly promote IGSCC of sensitized stainless steel. These species undergo cathodic reduction on the surface of the steel, which couples with anodic dissolution at the crack tip and leads to rapid advance of the stress corrosion crack. Apparently, the kinetics of the cathodic reduction process for these ions are higher than for other species at similar concentrations (e.g., dissolved oxygen or various oxyanions) since the crack growth rates are, in general, higher by a factor of 10 at a given strain rate and temperature. The dependence of the crack growth rates on the measured effluent copper concentrations is being evaluated in relation to the solubilities of Cu°, Cu^{+}, and Cu^{2+} and calculated pH values at the test temperatures. The experimental and calculated results will be presented in the next semiannual progress report.

Table 11. Influence of Temperature and Cu^+ Concentration on the SCC Susceptibility of Sensitized Type 304 SS Specimens[a] in Water Containing CuCl at a Low (<5 ppb) Dissolved-Oxygen Concentration

		Feedwater Chemistry					CERT Parameters	
		Cation Concentration						
Test No.	Temp., °C	Influent, ppm	Effluent,[b] ppm	Anion Conc., ppm	Cond. at 25°C, µS/cm	pH at 25°C	Failure Time, h	Maximum Stress, MPa
237	135	2.0	1.53	1.10	7.60	5.90	67	406
228	150	0.1	0.09	0.06	0.68	6.20	154	520
220	150	0.3	0.22	0.17	1.41	6.14	150	534
229	150	0.8	0.66	0.45	3.30	6.07	66	432
232	150	2.0	1.23	1.10	7.60	6.26	77	420
243	170	0.02	0.02	0.01	0.36	6.29	146	504
238	170	0.05	0.05	0.03	0.46	6.18	89	440
234	170	2.0	1.05	1.10	7.50	5.98	36	310
231	200	0.02	0.06	0.01	0.44	6.31	81	430
227	200	0.05	0.05	0.03	0.49	6.22	91	483
212	200	0.1	0.15	0.06	0.66	6.60	63[e]	504
223	200	0.1	0.07	0.06	0.63	6.25	89	476
219	200	0.3	0.38	0.17	1.43	6.26	85	447
213	200	0.5	0.55	0.28	2.30	5.97	95	476
230	200	0.5	0.42	0.28	2.10	6.08	39	297
214	200	0.8	0.76	0.45	3.60	6.00	47	298
211	200	1.0	0.94	0.55	4.40	5.92	25	254
226	200	2.0	0.90	1.10	7.70	5.94	24	245
233	250	2.0	0.78	1.10	7.50	6.31	33	256
215	289	0.8	0.52	0.45	3.50	5.87	147	534
216	289	2.0	0.73	1.10	7.90	5.86	152	529
217	289	5.0	1.46	2.75	20.0	5.98	139	527
218	289	10.0	3.65	5.50	38.0	6.23	28	249

[a] Lightly sensitized (EPR = 2 C/cm^2) specimens (Heat No. 30956) were exposed to the environments for ~20 h before being strained at a rate of 1 x 10^{-6} s^{-1}.

[b] Copper concentration of the effluent water was determined by inductively-coupled-plasma (ICP) spectrophotometry analyses.

[c] Ductile (D), transgranular (T), granulated (G), and intergranular (I), in terms of the fraction of the cross-sectional area. Characterization of the fracture surface morphologies is in accordance with the illustrations and definitions in Reference 35.

3.2.2
Effect of Organic Impurities on SCC (W. E. Ruther, W. K. Soppet, and T. F. Kassner)

Organic contaminants can enter BWR reactor coolant and PWR secondary-system water primarily through the radwaste floor drain sump system[39] and via the make-up water,[40] respectively. These substances or their decomposition products could influence the corrosion behavior or SCC susceptibility of system materials. Organic acids and salts along with chelating agents are routinely used in the decontamination of reactor components before in-service inspection and repair work,[41] and in the chemical cleaning of corrosion products and impurity deposits that accumulate at the tube sheet and tube support plates and in crevices between the tubes and support plates in PWR steam generators.[42] Numerous corrosion and SCC studies have been performed to qualify the various reagents and processes for use in nuclear power plants.[43-54] A summary of this work has been the topic of a recent review.[55,56]

CERT Parameters				Potentials		
Total Elong., %	Reduction in Area, %	Fracture Morphology[c]	SCC Growth Rate,[d] $m \cdot s^{-1}$	Type 304 SS, mV(SHE)	Pt, mV(SHE)	Cu, mV(SHE)
24	45	0.49D, 0.51I	8.2×10^{-9}	264	220	237
55	81	1.00D	-	229	-156	-112
54	81	1.00D	-	208	54	-34
24	47	0.42D, 0.58G_3	9.6×10^{-9}	305	287	-37
28	34	0.36D, 0.64I	8.9×10^{-9}	278	224	-18
53	81	1.00D	-	38	-331	-186
32	45	0.59D, 0.41I	7.2×10^{-9}	141	-349	-101
13	21	0.06D, 0.94I	3.2×10^{-8}	301	245	-67
30	45	0.57D, 0.43I	5.2×10^{-9}	130	-316	-225
33	41	0.67D, 0.33G_3	3.4×10^{-9}	53	-351	-245
52	76	1.00D	-	83	-229	-123
32	41	0.64D, 0.36G_3	4.3×10^{-9}	116	-360	-142
31	54	0.31D, 0.69G_3	8.1×10^{-9}	22	-256	-126
34	60	0.67D, 0.33G_3	5.4×10^{-9}	116	-41	-153
14	31	0.25D, 0.75I	2.6×10^{-8}	219	-92	-168
17	20	0.10D, 0.90I	2.8×10^{-8}	193	33	-145
9	18	0.14D, 0.86I	5.2×10^{-8}	220	68	-97
9	16	0.04D, 0.96I	5.1×10^{-8}	246	128	-98
12	10	0.17D, 0.83I	3.5×10^{-8}	87	-237	-241
53	58	0.88D, 0.12T	1.1×10^{-9}	-403	-351	-367
55	65	0.84D, 0.16T	1.1×10^{-9}	-381	-329	-355
50	41	0.77D, 0.23G_3	6.0×10^{-9}	-296	-286	-294
10	11	0.02D, 0.98G_3	4.7×10^{-8}	-246	-235	-240

[d] SCC growth rates are based on measurement of (1) the depth of the longest crack in an enlarged micrograph of the fracture surface and (2) the time period from the onset of yield to the point of maximum load on the tensile curve.

[c] Strain rate was $2.3 \times 10^{-6}\ s^{-1}$.

As part of our investigation of the effects of 1 ppm of several organic acids on the SCC of sensitized Type 304 SS in oxygenated water, CERT tests were performed on the steel in water containing 0.2 ppm dissolved oxygen and four EDTA salts at an anion concentration of 1 ppm. The results in Table 12 indicate that the transgranular crack growth rates of the steel in water containing two of the salts are very low (~3×10^{-10} $m \cdot s^{-1}$), and in the case of the other two, the values (~1.6×10^{-9} $m \cdot s^{-1}$) are an order of magnitude lower than in high-purity oxygenated water.[57] In contrast to the previous experiments,[57] the effluent dissolved-oxygen concentrations of the water were <5 ppb and the ECP values of the steel and the platinum and copper electrodes were also quite negative [-510 to -680 mV(SHE)]. Apparently these substances react with dissolved oxygen in the feedwater at high temperatures and thereby decrease the susceptibility of the steel to IGSCC. The carboxylic (acetic, formic, lactic, and oxalic) and short-chain aliphatic (propionic and butyric) acids at an anion concentration of 1 ppm did not react with dissolved oxygen in the feedwater on the basis of measurements on the effluent water and the ECP values of the steel [~0 to 100 mV(SHE)]; however, several of these

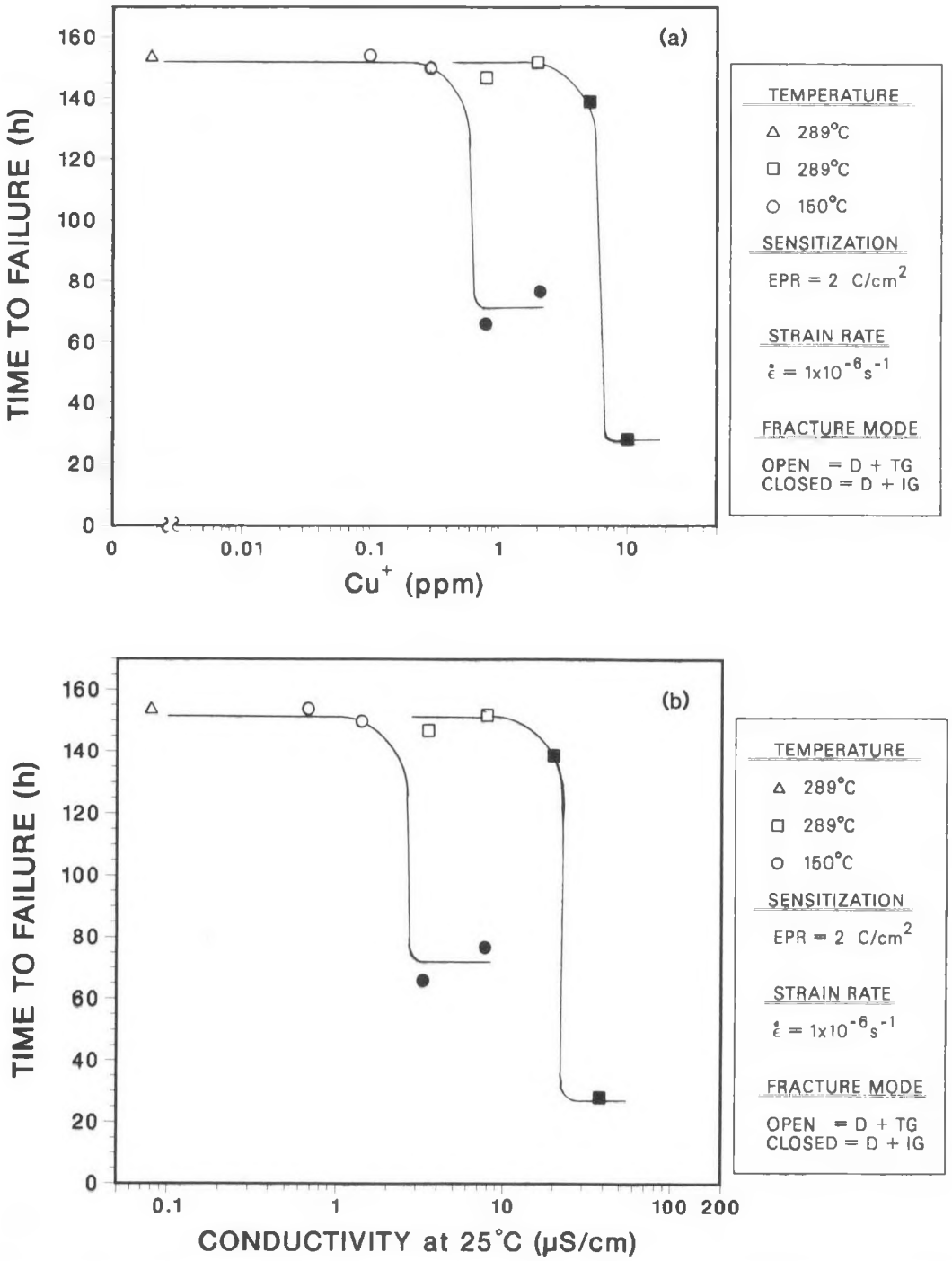

Figure 15. Dependence of the Time to Failure of Lightly Sensitized Type 304 SS Specimens (EPR = 2 C/cm^2) on (a) Cuprous Ion Concentration and (b) Conductivity of the Low-Oxygen (<5 ppb) Feedwater in CERT Experiments at 150 and 289°C.

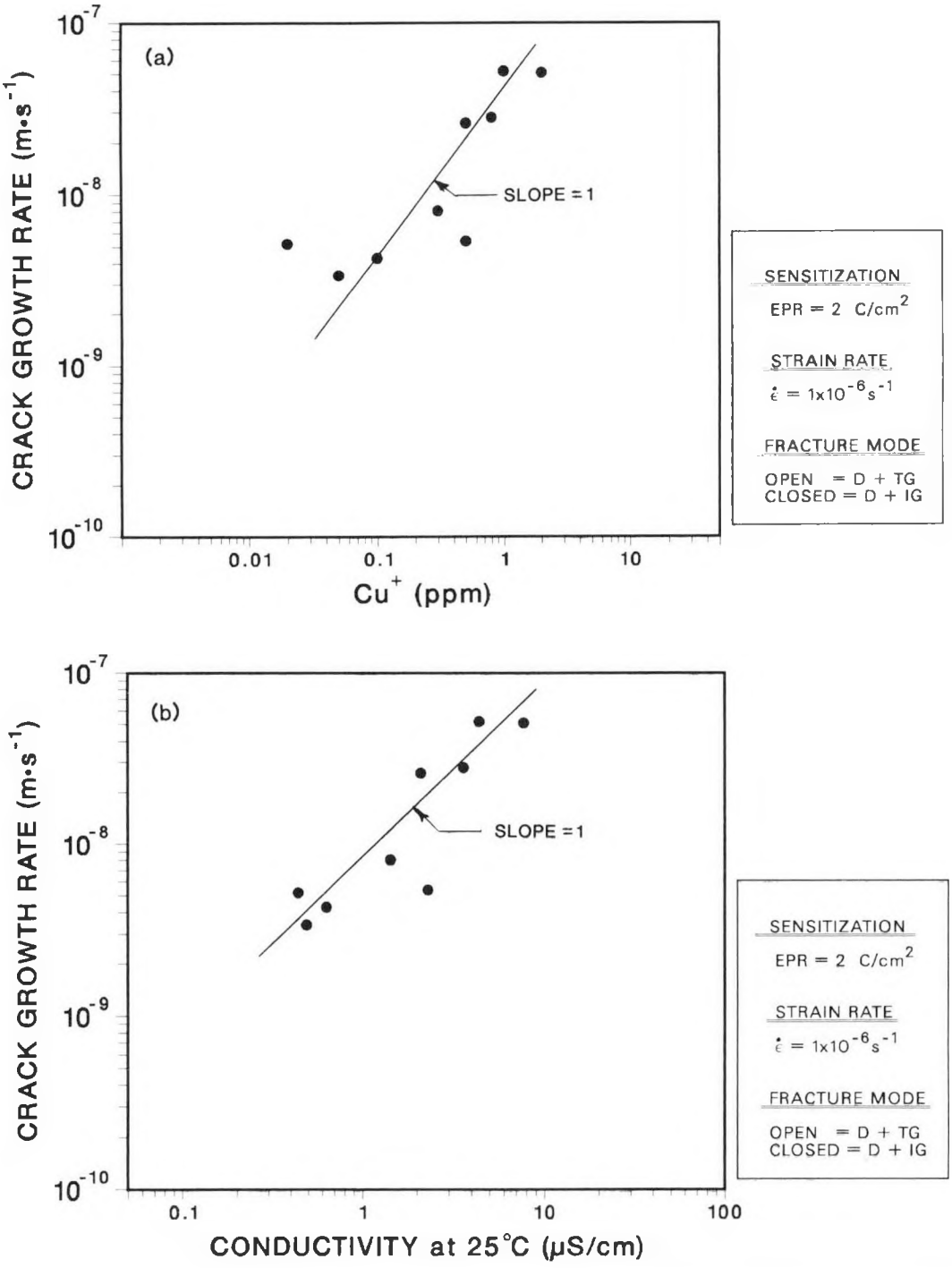

Figure 16. Dependence of the Crack Growth Rate of Lightly Sensitized Type 304 SS Specimens (EPR = 2 C/cm^2) on (a) Cuprous Ion Concentration and (b) Conductivity of the Low-Oxygen (<5 ppb) Feedwater in CERT Experiments at 200°C.

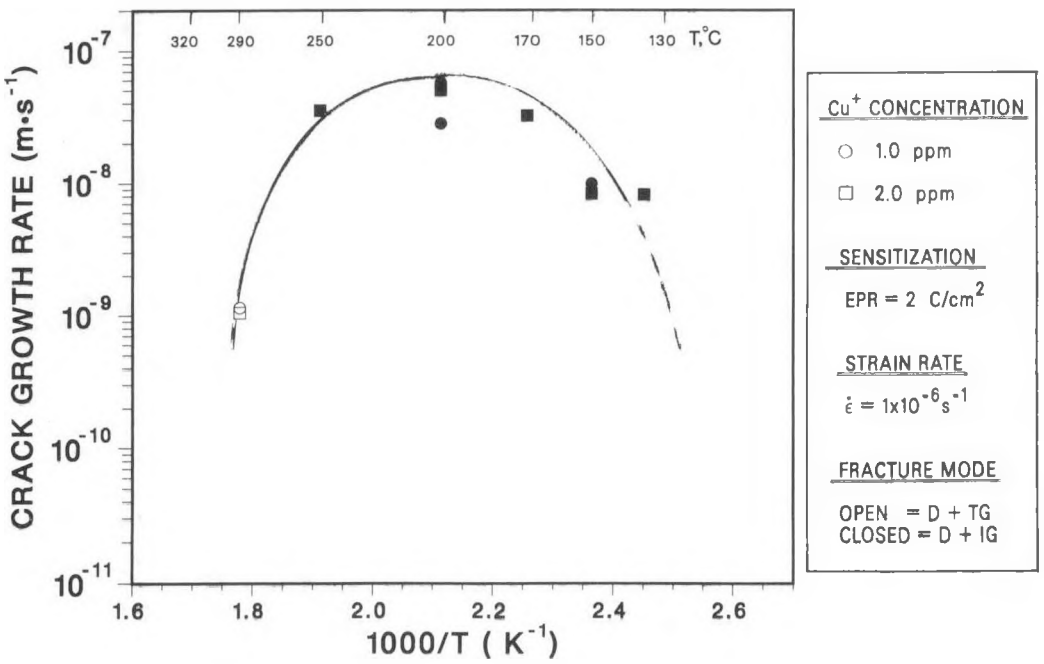

Figure 17. Effect of Temperature on the Crack Growth Rate of Lightly Sensitized Type 304 SS Specimens (EPR = 2 C/cm²) from CERT Experiments in Low-Oxygen (<5 ppb) Feedwater Containing ~1-2 ppm Cuprous Ion as CuCl.

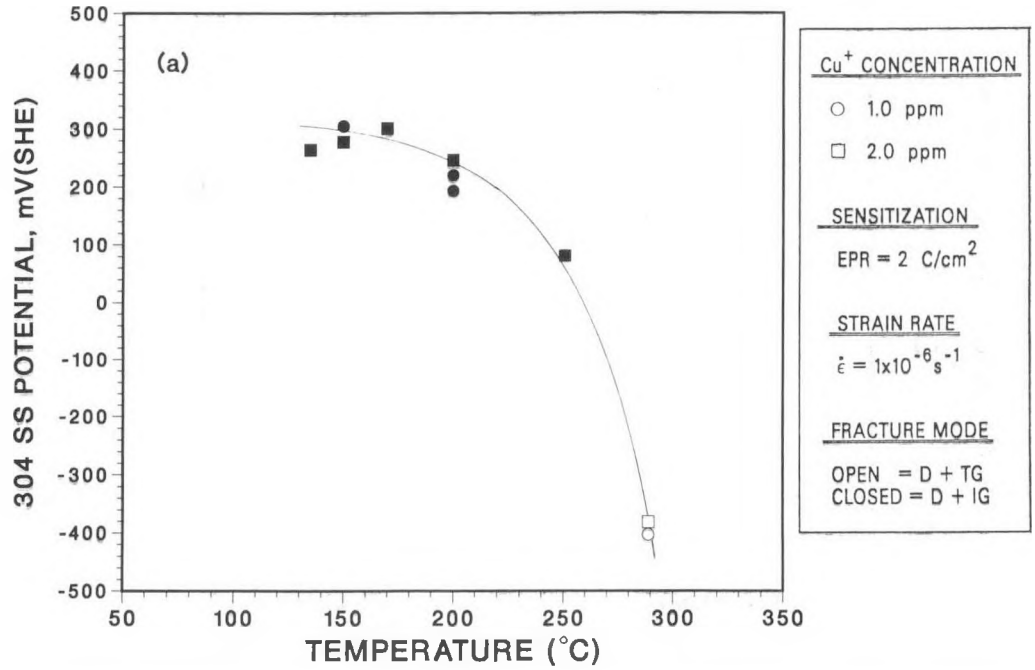

Figure 18. Temperature Dependence of the Steady-State Electrochemical Potential of (a) Type 304 SS, (b) Platinum, and (c) Copper during CERT Experiments on Lightly Sensitized Type 304 SS Specimens in Low-Oxygen (<5 ppb) Water Containing ~1-2 ppm Cuprous Ion as CuCl.

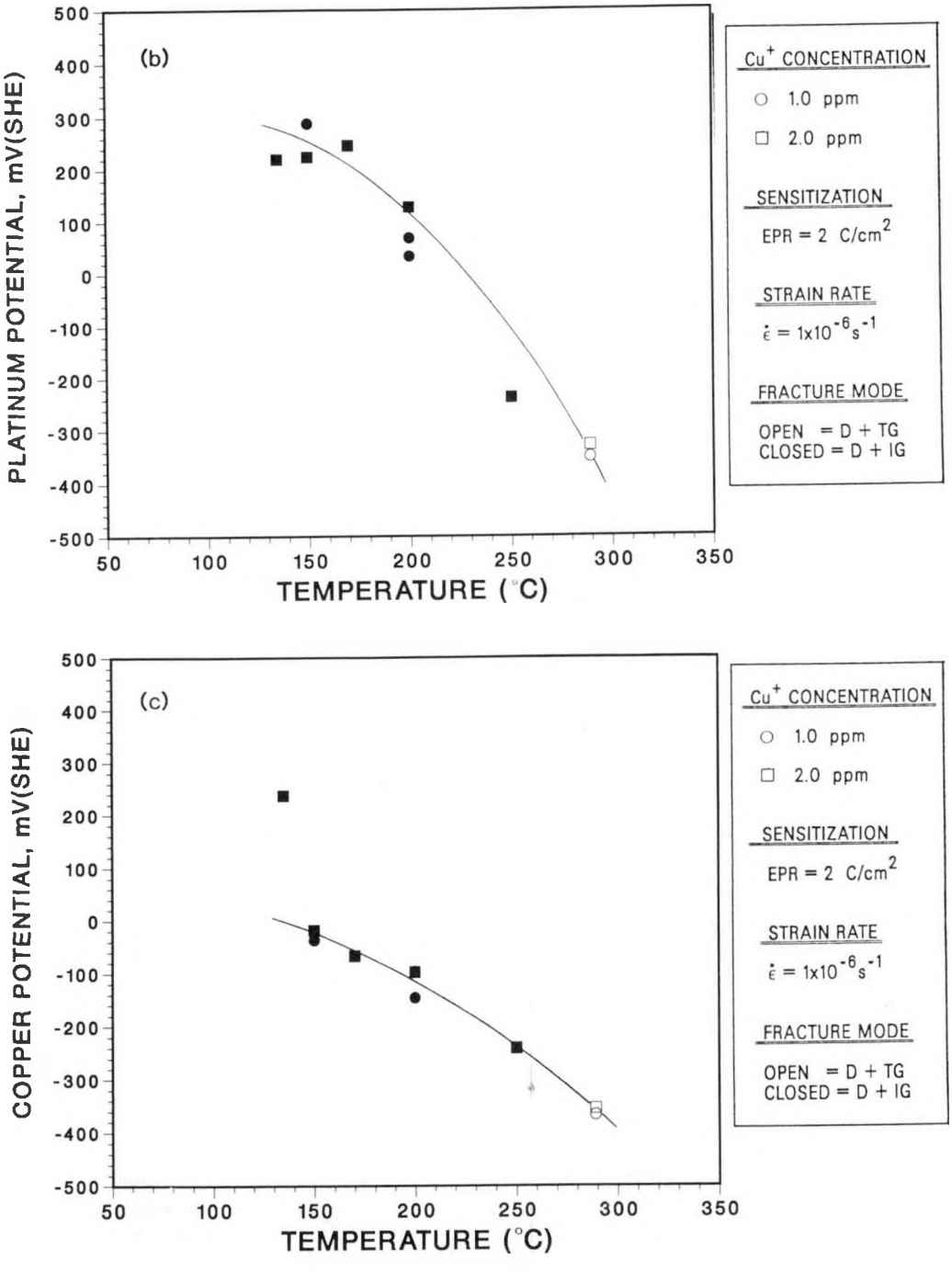
(b)
PLATINUM POTENTIAL, mV(SHE)
TEMPERATURE (°C)
Cu+ CONCENTRATION
1.0 ppm
2.0 ppm
SENSITIZATION
EPR = 2 C/cm2
STRAIN RATE
ε̇ = 1x10-6s-1
FRACTURE MODE
OPEN = D + TG
CLOSED = D + IG
(c)
COPPER POTENTIAL, mV(SHE)
TEMPERATURE (°C)
Cu+ CONCENTRATION
1.0 ppm
2.0 ppm
SENSITIZATION
EPR = 2 C/cm2
STRAIN RATE
ε̇ = 1x10-6s-1
FRACTURE MODE
OPEN = D + TG
CLOSED = D + IG

Fig. 18. (Contd.)

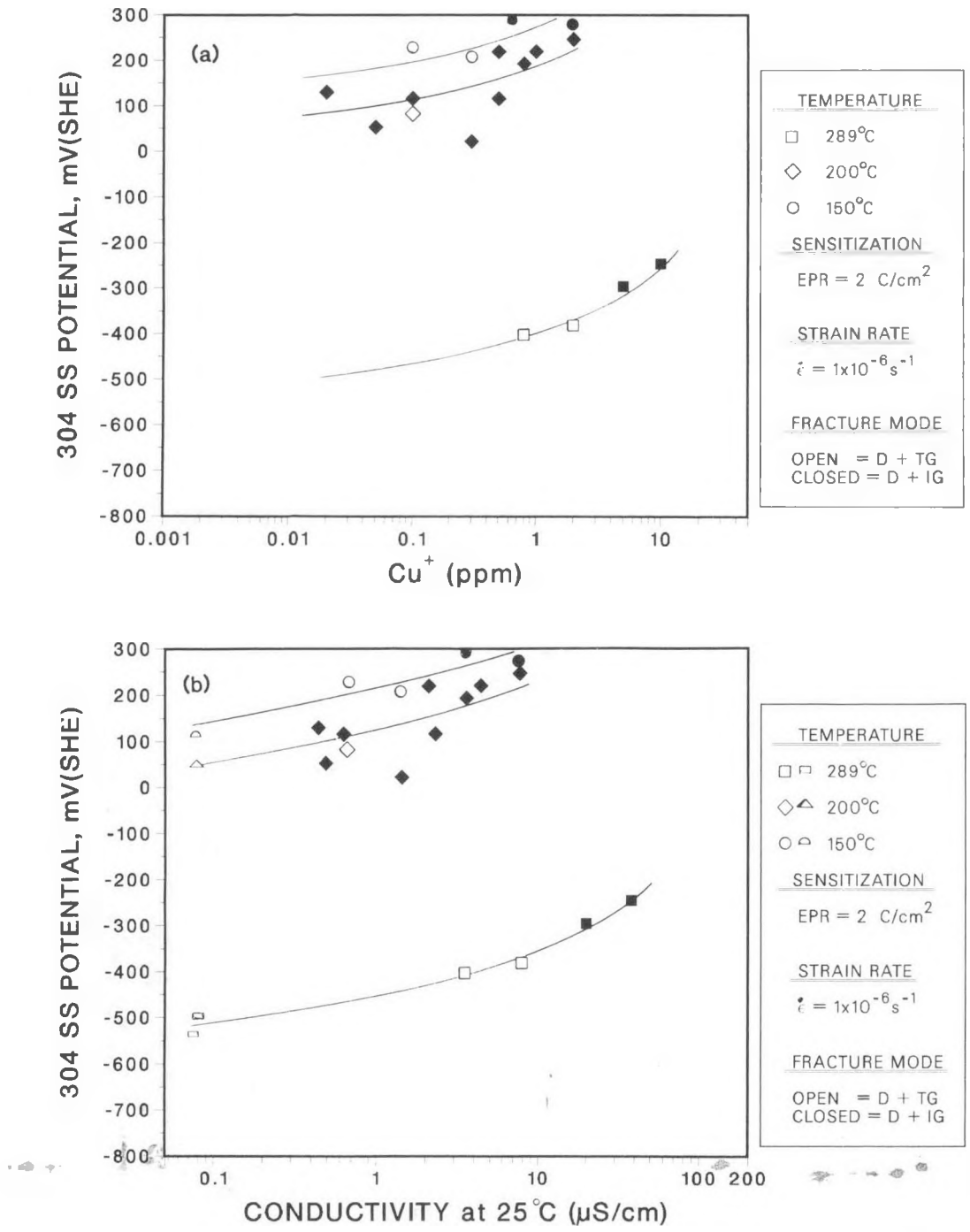

Figure 19. Dependence of the Steady-State Electrochemical Potential of Type 304 SS on (a) Cuprous Ion Concentration and (b) Conductivity of the Low-Oxygen (<5 ppb) Feedwater during CERT Experiments on Sensitized Type 304 SS Specimens at 150, 200, and 289°C. CERT specimens were not strained in the low-conductivity (<0.1 µS/cm) environments (no Cu^+ added to the feedwater), i.e., only ECP measurements were made over a time period of ~30 h at each temperature.

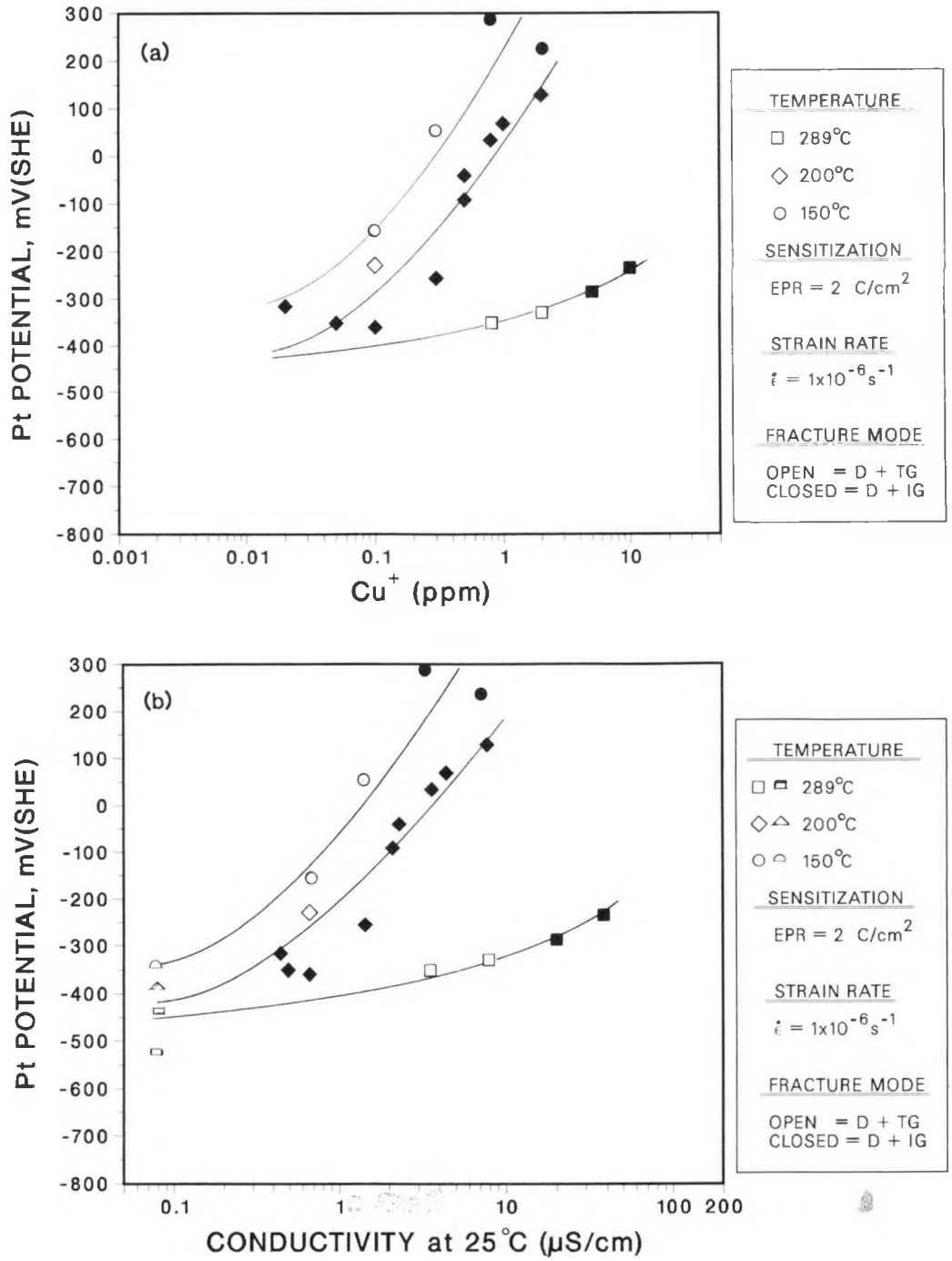

Figure 20. Dependence of the Steady-State Electrochemical Potential of Platinum on (a) Cuprous Ion Concentration and (b) Conductivity of the Low-Oxygen (<5 ppb) Feedwater during CERT Experiments on Sensitized Type 304 SS Specimens at 150, 200, and 289°C. CERT specimens were not strained in the low-conductivity (<0.1 µS/cm) environments (no Cu^+ added to the feedwater), i.e., only ECP measurements were made over a time period of ~30 h at each temperature.

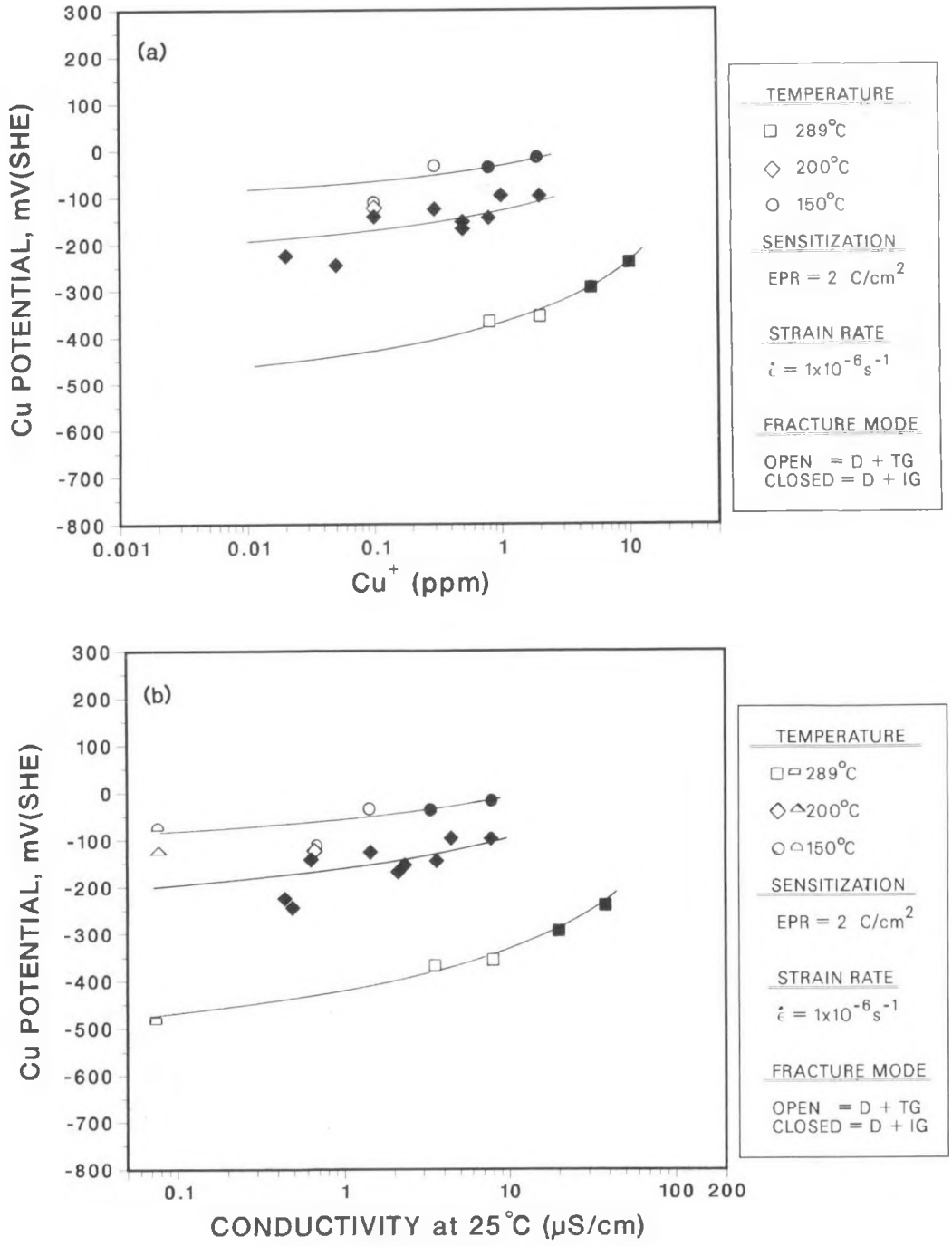

Figure 21. Dependence of the Steady-State Electrochemical Potential of Copper on (a) Cuprous Ion Concentration and (b) Conductivity of the Low-Oxygen (<5 ppb) Feedwater during CERT Experiments on Sensitized Type 304 SS Specimens at 150, 200, and 289°C. CERT specimens were not strained in the low-conductivity (<0.1 µS/cm) environments (no Cu^+ added to the feedwater), i.e., only ECP measurements were made over a time period of ~30 h at each temperature.

species decreased the crack growth rates of the steel significantly.[57]

Fracture-mechanics crack-growth-rate tests are in progress on sensitized Type 304 SS and Type 316NG SS specimens to confirm the relatively innocuous or potentially beneficial effects of several of the organic acids on SCC in water at 289°C containing 0.2 ppm dissolved oxygen. Initial results indicate that 1 ppm of propionic acid in the feedwater decreased the crack growth rate of the sensitized Type 304 SS specimen by an order of magnitude under low-frequency, high-R loading conditions at a maximum stress intensity value of ~30 MPa·m$^{1/2}$; however, the crack growth in the Type 316NG SS specimen continued at the same rate as in high-purity water.

3.2.3 Effect of Hydrogen-Water Chemistry on Crack Initiation and Growth (P. S. Maiya)

As reported previously,[58] crack initiation results for solution-annealed and sensitized Type 304 and nonsensitized Type 316NG SS indicated that crack initiation occurs at plastic strains of <4.0%, <2.0%, and <3.0%, respectively, in water containing 0.25 ppm dissolved oxygen and 0.1 ppm sulfate at 289°C. Thus, stress corrosion crack initiation occurs at relatively low plastic strains in all the materials, although solution-annealed Type 304 SS appears to be somewhat more resistant to crack initiation. A reduction in dissolved oxygen concentration or ECP improves the crack growth resistance of both Types 316NG and 304 SS.[59,60] To determine whether this condition also improves resistance to crack initiation, CERT experiments were performed on solution-annealed Type 304 SS in water containing between 0.005 and 0.25 ppm dissolved oxygen and 0.1 ppm sulfate, corresponding to ECP values ranging from -560 to 100 mV (SHE). The specimens in these tests had small holes drilled in the gage section to localize the cracking.[58] The tests were interrupted after various nominal plastic strains, ε_{nom}, between 0.2 and 1.0%, and the specimens were cross-sectioned to observe crack initiation by SEM, as described in an earlier report.[58]

Figure 22 shows the effect of ECP on the local plastic strain, ε_{loc}, required for crack initiation. The local plastic strain is assumed to be ~8 times the nominal strain, as in previous analytical studies.[58] The square and round symbols represent the presence and absence of SCC, respectively. Even at potentials below -400 mV (SHE), SCC initiates at strains of ~4.0%. This behavior is similar to that in oxygenated environments, i.e., crack initiation is relatively unaffected by the low corrosion potential.

Tests were also performed to determine the effect of low dissolved-oxygen levels or ECP values on crack growth rates in solution-annealed Type 304 SS. Experiments were performed in water containing 0.1 ppm sulfate along with 0.25 and 0.005 ppm dissolved oxygen, which correspond to ECP values of ~20 and -504 mV(SHE), respectively. As shown in Fig. 23, the crack growth rates are fairly insensitive to dissolved-oxygen level. This finding is reasonably consistent with our previous fracture-mechanics crack-growth tests on solution-annealed Type 304 SS,[61] in which the dissolved-oxygen levels (ECP values) required to arrest crack growth in solution-annealed material were lower than those for sensitized material.

The effect of strain rate on SCC has been studied under normal BWR-type water chemistry conditions,[5,62-64] but less information is available for simulated hydrogen water chemistry conditions. The results in Fig. 23 suggest that the dependence of crack growth rate of

Table 12. Influence of Several EDTA Salts[a] in Feedwater with 0.2 ppm Dissolved Oxygen[b] on the SCC Susceptibility of Sensitized Type 304 SS Specimens[c] at 289°C

	Feedwater Chemistry			CERT Parameters			
Test No.	Species[a]	Anion Conc., ppm	Cond. at 25°C, μS/cm	pH at 25°C	Failure Time, h	Maximum Stress, MPa	Total Elong., %
A162	4Na-EDTA	1.0	1.71	7.55	239	522	45
A164	Hydroxy-EDTA	1.0	1.95	5.41	243	526	46
A165	Cu,2Na-EDTA	1.0	0.91	6.17	277	534	52
A163	Fe,Na-EDTA	1.0	0.62	6.16	295	532	55

[a]Ethylenediaminetetraacetate (EDTA) salts in the experiments were as follows: 4Na·EDTA·$3H_2O$; N-(2-hydroxyethyl)·EDTA acid; Cu,2Na·EDTA·$2H_2O$; and Fe,Na·EDTA·$2H_2O$.

[b]Effluent dissolved-oxygen concentration determined by Chemetrics analyses was <5 ppb.

[c]Lightly sensitized (EPR = 2 C/cm^2) specimens (Heat No. 30956) were exposed to the environments for ~20 h before being strained at a rate of 5.2×10^{-7} s^{-1}.

solution-annealed Type 304 SS on strain rate is relatively independent of the corrosion potential. A power-law fit to the data in Fig. 23 yields an exponent of ~1/3, which is consistent with our modeling studies and previous results on sensitized Type 304 and Type 316NG SS.[5,62] The values of these exponents are consistent with the hypothesis that the crack growth rate is environmentally assisted even under low-ECP conditions (since applied creep effects are unlikely to be important at the temperature and strain rates in this study).

4 Environmentally Assisted Cracking of Ferritic Steels

4.1 Introduction

Plain carbon steels are used extensively in PWR and BWR nuclear steam supply systems as piping and pressure vessel materials. The steels of interest for these applications include grade A106-Gr B and A333-Gr 6 for seamless pipe and A302-Gr B, A508-2, and A533-Gr B plate for pressure vessels. Although operating experience with ferritic steel components in reactor pressure boundaries is considerably better than with weld-sensitized austenitic stainless steels, instances of cracking of these steels have occurred in the U.S. and abroad.[65-73]

Ferritic steels have been shown to become susceptible to TGSCC in high-temperature water containing dissolved oxygen in CERT[74-81] and fracture-mechanics tests.[82-88] There is some evidence of synergistic effects between dissolved oxygen and soluble copper compounds (viz., $CuCl_2$) as well as other impurities to produce susceptibility to SCC.[70,76] However, the ranges of dissolved-oxygen and impurity concentrations that can lead to SCC in these materials remain

CERT Parameters			Potentials[c]		
Reduction in Area, %	SCC Growth Rate,[d] $m \cdot s^{-1}$	Fracture Morphology[e]	Type 304 SS, mv(SHE)	Pt, mv(SHE)	Cu, mV(SHE)
48	1.6×10^{-9}	0.46D, 0.54T	-682	-601	-508
44	1.6×10^{-9}	0.77D, 0.23T	-612	-570	-658
57	3.1×10^{-10}	0.96D, 0.04T	-518	-543	-526
74	3.1×10^{-10}	0.86D, 0.14T	-586	-573	-592

[d]SCC growth rates are based on measurement of the depth of the longest crack in an enlarged micrograph of the fracture surface and the time period from the onset of yield to the point of maximum load on the tensile curve.

[e]Ductile (D) and transgranular (T), in terms of the fraction of the cross-sectional area. Characterization of the fracture surface morphologies is in accordance with the illustrations and definitions in Reference 35.

relatively ill-defined. The objective of this work is to characterize the environmental and material conditions that can produce SCC susceptibility in these steels.

4.2 Technical Progress

4.2.1 Constant Extension Rate Tests (J. Y. Park)

CERT tests were continued on unnotched cylindrical gage-length specimens fabricated from several ferritic steels (A333, A106, A155, A516, and A533B). These materials have been used in other USNRC research programs at Battelle Columbus Laboratories and Materials Engineering Associates, Inc., and have been well characterized in terms of mechanical properties. The chemical composition of the materials was presented in a previous report.[89] The tests were performed in oxygenated water at 289°C without and with 0.01 and 0.1 ppm sulfate additions (as H_2SO_4) at strain rates of 1.0×10^{-6} and 2.5×10^{-7} s^{-1}. The dissolved-oxygen concentration was 0.2–0.3 ppm, except for one test that was run at 0.5 ppm. In order to maintain good control of the dissolved-oxygen concentration, all areas of the autoclave and water supply system in contact with high-temperature water were fabricated from titanium. The test specimens were electrically isolated from the load train and autoclave, and electrochemical potential was continually monitored.

The results of the CERT tests are summarized in Table 13. All heats of materials showed transgranular cracking on the fracture surfaces, except for one heat of A533B (Heat No. A5401, specimen No. W7-

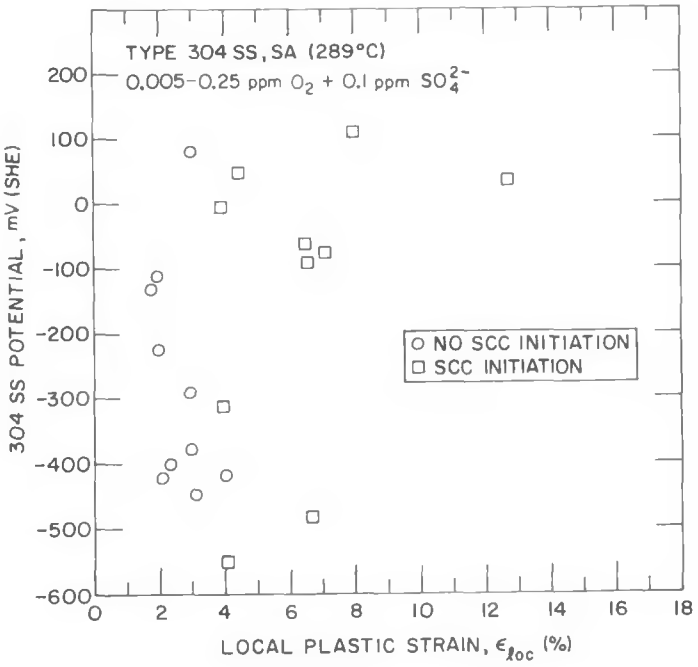

Figure 22.
Effect of Open-Circuit Electrochemical Potential on Crack Initiation in Solution-annealed (SA) Type 304 SS. The local plastic strain is computed by use of a strain concentration factor of ~8.

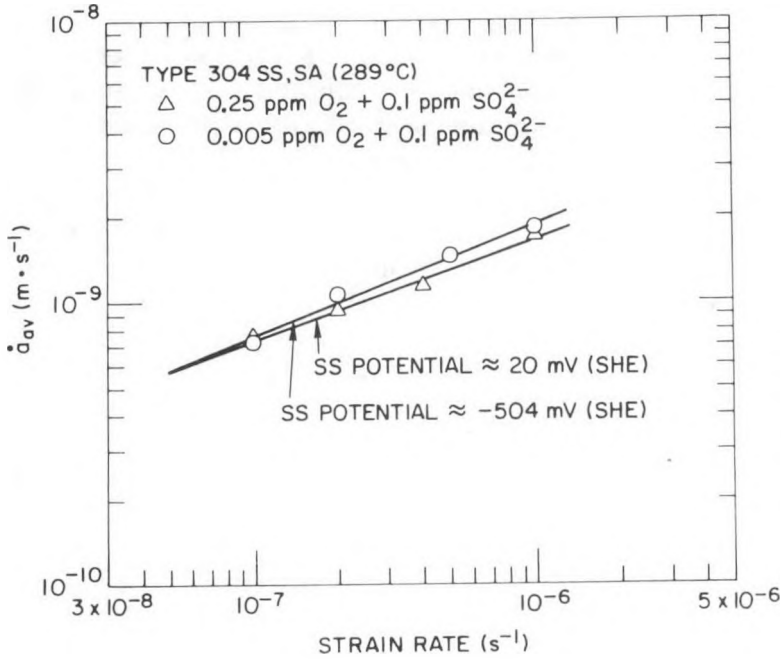

Figure 23.
Effect of Oxygen or Electrochemical Potential on Crack Growth Rates of Solution-annealed (SA) Type 304 SS.

Table 13. Results of CERT Tests[a] on Ferritic Steels in Oxygenated Water at 289°C

Material and Heat No.	Specimen No.	Max. Load, MPa	t_f, h	RA, %	Elong., %	$\dot{a}_{av}$, $m \cdot s^{-1}$	ECP, mV(SHE)
			High-Purity Water with 0.2–0.3 ppm Oxygen				
A533B A5401	W7-2	657	63.7	72.5	22.0	1.4×10^{-10}	-40
A533B XE5-M	5M-2	614	55.6	71.7	23.5	6.4×10^{-9}	+40
A516 GR70 DP2-F34	34-2A	507	95.9	78.8	40.4	1.5×10^{-10}	-40
A155-CK70 DP2-F26	26-2	527	82.6	49.8	28.3	1.2×10^{-9}	0
A106B DP2-F29	29B-2	570	75.2	57.6	28.5	1.4×10^{-10}	-
A106B DP2-F30	30C-3	640	76.7	29.8	28.4	4.6×10^{-9}	-20
"	30C-1	626	47.4	16.5	17.6	3×10^{-8}	+50
"	30C-2[b]	632	291.7	39.3	29.2	3×10^{-9}	-20
			High-Purity Water with 0.5 ppm Oxygen				
A106B DP2-F30	30C-4	627	68.0	15.5	27.4	2.8×10^{-9}	+110
			Water with 0.01 ppm Sulfate and 0.2–0.3 ppm Oxygen				
A106B DP2-F29	29B-6	554	81.3	42.0	28.4	-	-75
A106B DP2-F30	30C-6	619	70.5	46.3	22.5	4.2×10^{-9}	-110
			Water with 0.1 ppm Sulfate and 0.2–0.3 ppm Oxygen				
A106 B DP2-F29	29B-5	472	68.7	41.6	34.5	3.9×10^{-9}	-170
"	29B-7	554	60.9	29.9	21.9	5.9×10^{-9}	-
A106 B DP2-F30	30C-7	624	66.8	63.2	25.8	6.2×10^{-9}	-
"	30C-8	620	71.1	39.1	24.8	7.2×10^{-9}	-188
A533 B A5401	W7-3	646	61.2	65.9	25.8	Ductile	-68
A533 B XE5-M	5M-3	593	43.5	42.3	20.9	1.0×10^{-8}	-70
A155-CK70 DP2-F26	26-3	514	64.4	38.8	26.4	6.0×10^{-9}	-63

[a]Strain rate was 1×10^{-6} s^{-1}, except where noted.
[b]Strain rate was 2.5×10^{-7} s^{-1}.

3) that was tested in water containing 0.2–0.3 ppm oxygen and 0.1 ppm sulfate. An average crack growth rate was calculated by dividing the maximum crack depth by the time to maximum load. As shown in Table 13, the average crack growth rates varied widely (from 1×10^{-10} to 3×10^{-8} $m \cdot s^{-1}$), even for the same heat of material. There was no significant difference in crack growth rate between the tests in the water with 0.2–0.3 ppm and 0.5 ppm oxygen. The growth rate for the A106B steel (Heat No. DP2–F30) in water with 0.2–0.3 ppm oxygen varied from 3×10^{-9} to 3×10^{-8} $m \cdot s^{-1}$, whereas the rate in water with 0.5 ppm oxygen was 3×10^{-9} $m \cdot s^{-1}$. Future tests with dissolved-oxygen concentrations of less than 30 ppb are planned.

As expected from related work on the fatigue crack growth of ferritic steels in reactor environments,[90,91] there appears to be a strong correlation between the sulfur content of the steel (particularly the presence of sulfide inclusions) and susceptibility to SCC. The fracture surface of specimen 30C–1 (A106B Heat DP2–30, Fig. 24) shows brittle transgranular SCC. The fracture surface of specimen W7–3 (A533B, Heat No. A5401, Fig. 25) shows ductile fracture without SCC. Figures 26 and 27 are micrographs of the cross sections of specimens 30C–1 and W7–3, respectively. There are far fewer inclusions in the less susceptible A533B steel than in the more susceptible A106B material. Nonuniform distributions of inclusions may also be responsible for the specimen-to-specimen variation in crack growth rates in the same heat of material.

The addition of 0.1 ppm sulfate does not seem to have an appreciable effect on crack growth rates in these materials. Presumably, crack tip impurity levels from the inclusions overwhelm the contributions from the bulk water chemistry.

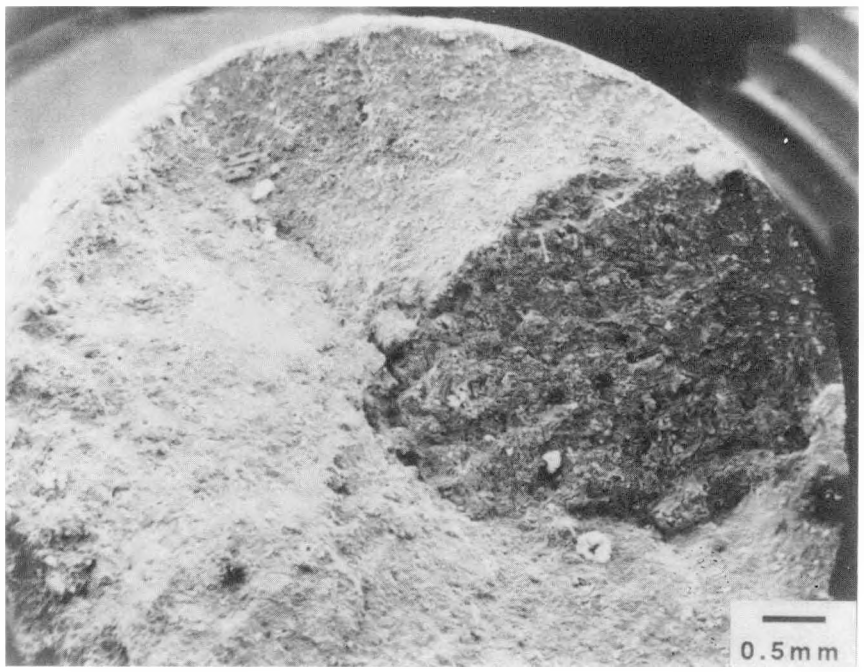

Figure 24. Fracture Surface of A106B Ferritic Steel (Heat No. DP2–F30, Specimen No. 30C–1) after a CERT Test in Water with 0.2–0.3 ppm Oxygen at 289°C. Transgranular cracking is evident.

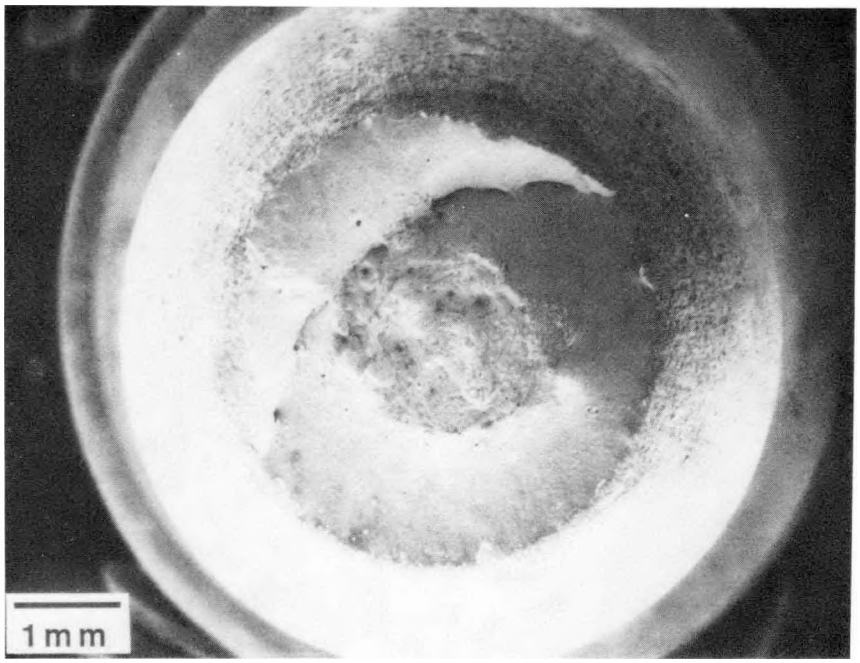

Figure 25. Fracture Surface of A533B Ferritic Steel (Heat No. A5401, Specimen No. W7–3) after a CERT Test in Water with 0.1 ppm Sulfate and 0.2–0.3 ppm Oxygen at 289°C. No transgranular cracking is evident.

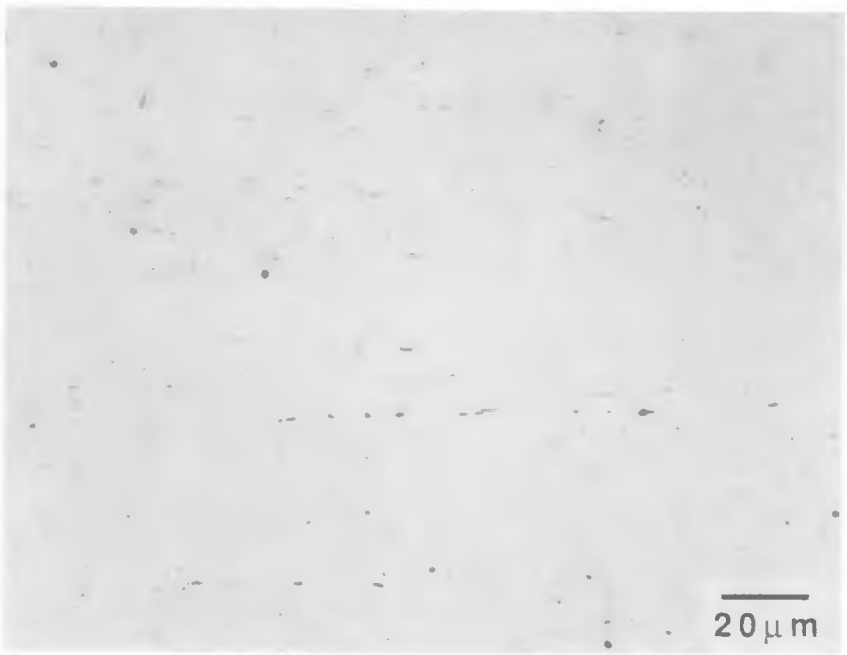

Figure 26. Longitudinal Cross Section of A106B Ferritic Steel (Heat No. DP2–F30, Specimen No. 30C–1) Showing Distribution of Inclusions.

Figure 27. Longitudinal Cross Section of A533B Ferritic Steel (Heat No. A5401, Specimen No. W7–3) Showing Distribution of Inclusions.

References

1. W. E. Ruther, W. K. Soppet, J. Y. Park, and T. F Kassner, in *Environmentally Assisted Cracking in Light Water Reactors: Semiannual Report, April–September 1986*, NUREG/CR–4667 Vol. III, ANL–87–37 (September 1987) pp. 1–7.

2. M. T. Jones, *Reactor Technology Report*, Knolls Atomic Power Laboratory, No. KAPL 2000–11 (1960).

3. W. E. Ruther and S. Greenberg, "Corrosion of Steels and Nickel Alloys in Superheated Steam," *J. Electrochem. Soc.* **111**, 1116–1121 (1964).

4. W. E. Ruther, W. K. Soppet, and T. F. Kassner, in *Materials Science and Technology Division Light–Water–Reactor Safety Research Program: Quarterly Progress Report, October–December 1983*, NUREG/CR–3689 Vol. IV, ANL–83–85 Vol. IV (August 1984), pp. 75–87.

5. P. S. Maiya and W. J. Shack, in *Environmentally Assisted Cracking in Light Water Reactors: Semiannual Report, April–September 1985*, NUREG/CR–4667 Vol. I, ANL–86–31 (June 1986), pp. 16–26.

6. P. S. Maiya, in *Environmentally Assisted Cracking in Light Water Reactors: Semiannual Report, April–September 1986*, NUREG/CR–4667 Vol. III, ANL–87–37 (September 1987), pp. 7–11.

7. A. J. Sedriks, *Corrosion of Stainless Steels*, John Wiley & Sons, New York (1979), pp. 145–150.

8. J. Bourrat and J. Hochmann, "Stress Corrosion in Austenitic Stainless Steel," *Mem. Sci. Rev. Metall.*, **60**, 551–563 (1963).

9. P. S. Maiya, in *Environmentally Assisted Cracking in Light Water Reactors: Semiannual Report October 1986–March 1987*, NUREG/CR–4667 Vol. IV, ANL–87–41 (December 1987), pp. 10–24.

10. D. L. Douglass, G. Thomas and W. R. Roser, "Ordering, Stacking Faults, and Stress Corrosion Cracking in Austenitic Alloys," in *Proc. 2nd Int. Cong. on Metallic Corrosion*, New York, N.Y., March 11–15, 1963, NACE, Houston (1963), pp. 66–79.

11. V. N. Shah and P. E. MacDonald, *Residual Life Assessment of Major Light Water Reactor Components–Overview Volume 1*, NUREG/CR-4731 EGG–2469 Vol. 1 (June 1987).

12. *ASME Boiler and Pressure Vessel Code, Section III Nuclear Power Plant Components*, 1983 Edition, American Society of Mechanical Engineers, New York (1983).

13. H. S. Mehta, S. Ranganath, and D. Weinstein, *Application of Environmental Fatigue Stress Rules to Carbon Steel Reactor Piping*, EPRI NP–4644M Vols. 1 and 2 (July 1986).

14. D. A. Hale, S. A. Wilson, E. Kiss, and A. J. Gianuzzi, *Low Cycle Fatigue Evaluation of Primary Piping Materials in a BWR Environment*, GEAP-20244 (September 1977).

15. J. B. Terrell, *Fatigue Life Characterization of Smooth and Notched Piping Steel Specimens in 288°C Environments*, NUREG/CR-5013 (May 1988).

16. J. Alexander et al., *Alternative Alloys for BWR Pipe Applications*, EPRI NP-2671-LD (October 1982), pp. 5-43 to 5-55.

17. *Criteria of the ASME Boiler and Pressure Vessel Code for Design by Analysis in Sections III and VIII, Division 2*, American Society of Mechanical Engineers, New York (1969).

18. W. E. Ruther, W. K. Soppet, and T. F. Kassner, in *Light-Water-Reactor Safety Materials Engineering Programs: Quarterly Progress Report, January-March 1985*, NUREG/CR-4490 Vol. I, ANL 85-75 Vol. I (March 1986), pp. 25-42.

19. W. E. Ruther, W. K. Soppet, and T. F. Kassner, in *Environmentally Assisted Cracking in Light Water Reactors: Semiannual Report, April-September 1985*, NUREG/CR-4667 Vol. I, ANL-86-31 (June 1986), pp. 27-41.

20. W. E. Ruther, W. K. Soppet, and T. F. Kassner, in *Environmentally Assisted Cracking in Light Water Reactors: Semiannual Report, April-September 1986*, NUREG/CR-4667 Vol. III, ANL-87-37 (September 1987), pp. 40-51.

21. W. E. Ruther, W. K. Soppet, and T. F. Kassner, in *Environmentally Assisted Cracking in Light Water Reactors: Semiannual Report, October 1986-March 1987*, NUREG/CR-4667 Vol. IV, ANL-87-41 (December 1987), pp. 35-47.

22. W. E. Bailey, M. O. Marlowe, and R. A. Proebstle, "Trends in BWR Fuel Performance," in *Light Water Reactor Fuel Performance*, Proc. Amer. Nucl. Soc. Topical Meeting, Orlando FL, April 21-24, 1985, Vol. 1, pp. 1-3 to 1-16.

23. M. O. Marlowe, J. S. Armijo, B. Cheng, and R. B. Adamson, "Nuclear Fuel Cladding Localized Corrosion," in *Light Water Reactor Fuel Performance*, Proc. Amer. Nucl. Soc. Topical Meeting, Orlando FL, April 21-24, 1985, Vol. 1, pp. 3-73 to 3-90.

24. A. K. Agrawal, J. F. Sykes, W. N. Stiegelmeyer, and W. E. Berry, "Pitting of Alloy 600 Steam Generator Tubes in Indian Point No. 3," in *Environmental Degradation of Materials in Nuclear Power Systems-Water Reactors*, Proc. Int. Symp., Myrtle Beach, SC, August 22-25, 1983, NACE, Houston (1984), pp. 223-242.

25. S. L. Harper, S. C. Inmann, P. L. Daniel, B. P. Miglin, and G. J. Theus, "Laboratory Evaluation of Steam Generator Tubes from Millstone Point Unit 2 and the Use of Pourbaix Diagrams to Infer Localized Corrosion Conditions," in *Environmental Degradation of Materials in Nuclear Power Systems-Water Reactors*, Proc. 2nd Int. Symp., Monterey, CA, September 9-12, 1985, NACE, Houston (1986), pp. 227-233.

26. S. J. Green and J. P. N. Paine, "Steam Generator Materials--Experience and Prognosis," in *Environmental Degradation of Materials in Nuclear Power Systems-Water Reactors*, Proc. Int. Symp., Myrtle Beach, SC, August 22-25, 1983, NACE, Houston (1984), pp. 53-68.

27. T. J. Zeh, G. O. Hayner, and A. K. Agrawal, "Intergranular Attack of Inconel 600 Tubes at Tube Support Plate Intersections in the Palisades Nuclear Power Plant," in *Environmental Degradation of Materials in Nuclear Power Systems-Water Reactors*, Proc. 2nd Int. Symp., Monterey, CA, September 9-12, 1985, NACE, Houston (1986), pp. 234-239.

28. D. D. Macdonald, A. K. Eghan, and Z. Szklarska-Smialowska, "Stress Corrosion Cracking of AISI 304 Stainless Steel in Oxygenated High Temperature Chloride Solutions Containing Cupric (Cu2+) and Lead (Pb2+) Ions," *Corrosion* (Houston) **41**, 474-484 (1985).

29. F. P. Ford, "Stress Corrosion Cracking," in *Corrosion Processes*, R. N. Parkins, ed., Applied Science Publishers, New York (1982), pp. 271-309.

30. D. A. Vermilyea, in *Proc. Int. Conf. on Stress Corrosion Cracking and Hydrogen Embrittlement of Iron Base Alloys*, R. W. Staehle, J. Hochmann, R. D. McCright, and J. E. Slater, eds., NACE, Houston (1983), p. 208.

31. *BWR Water Chemistry Guidelines*, Prepared by the BWR Owners Group Water Chemistry Guidelines Committee, EPRI NP-3589 SR-LD (April 1985), pp. 3-1 to 3-9.

32. *PWR Secondary Water Chemistry Guidelines, Revision 1*, Prepared by the Steam Generator Owners Group Water Chemistry Guidelines Revision Committee, EPRI NP-5056-SR (March 1987), pp. 2-12 to 2-22 and 3-15 to 3-22.

33. G. F. Palino, "Lessons Learned in the Vermont Yankee Project," in *Proc. 1986 Seminar on BWR Corrosion, Chemistry, and Radiation Control*, EPRI, Palo Alto, CA, November 10-12, 1986.

34. D. Cubicciotti, "Pourbaix Diagrams for Mixed Metal Oxides: The Chemistry of Copper in BWR Water," NACE *Corrosion/88*, St Louis, MO, March 1988, Paper No. 254.

35. H. D. Solomon, "Transgranular, Granulated, and Intergranular Stress Corrosion Cracking in AISI 304 SS," *Corrosion* (Houston) **40**, 493-506 (1984).

36. W. E. Ruther, W. K. Soppet, and T. F. Kassner, in *Light-Water-Reactor Safety Materials Engineering Research Programs: Quarterly Progress Report, January-March 1984*, NUREG/CR-3998 Vol I, ANL-84-60 (September 1984), pp. 38-49.

37. W. E. Ruther, W. K. Soppet, and T. F. Kassner, "Effect of Temperature and Ionic Impurities at Very Low Concentrations on Stress Corrosion Cracking of AISI 304 Stainless Steel," *Corrosion* (Houston) **44**, 791-799 (1988)..

38. W. E. Ruther, W. K. Soppet, and T. F. Kassner, in *Light-Water-Reactor Safety Materials Engineering Research Programs: Quarterly Progress Report, October-December 1984*, NUREG/CR-3998 Vol III, ANL-84-60 Vol. III (September 1984), pp. 24-36.

39. B. H. Dillman, J. C. Elliot, R. A. Head, J. E. Osterle, and R. S. Tunder, *Monitoring of Chemical Contaminants in BWRs, Final Report*, EPRI NP-4134 (July 1985).

40. J. E. Richards and W. A. Byers, *Industrywide Survey of PWR Organics, Final Report*, EPRI NP-4698 (July 1986).

41. C. J. Wood, "Decontamination Helps Control Nuclear-Maintenance Costs," *Power* **129**, 29-33 (1985).

42. N. R. Stolzenberg and R. C. Thomas, "Employing a Chemical Method for Tubesheet Sludge Removal," *Nucl. Eng, Int.* **32**, 29-41 (1987).

43. J. P. Michalko, P. J. Bonnici, and J. L. Smee, *Compilation of Corrosion Data on CAN-DECON™, Volume 1: General, Galvanic, Crevice, and Pitting Corrosion Data from CANDU and BWR Tests*, EPRI NP-4222 Vol. 1 (October 1985).

44. J. P. Michalko and J. L. Smee, *Compilation of Corrosion Data on CAN-DECON™, Volume 2: Influence of CAN-DECON on Stress Corrosion Cracking—Summary of Testing, 1975-1983*, EPRI NP-4222 Vol. 2 (October 1985).

45. P. J. King and B. D. Warr, *Compilation of Corrosion Data on CAN-DECON™, Volume 3: Influence of CAN-DECON Process on Stress Corrosion Cracking—1984 Constant-Extension-Rate Tests*, EPRI NP-4222 Vol. 3 (January 1987).

46. J. L. Smee and V. C. Turner, *Compilation of Corrosion Data on CAN-DECON™, Volume 4: General, Galvanic, Crevice, Pitting, and Stress Corrosion Data From PWR Tests and Applications*, EPRI NP-4222 Vol. 4 (January 1987).

47. J. L. Smee and V. C. Turner, *Compilation of Corrosion Data on CAN-DECON™, Volume 5: Influence of the CAN-DECON™ Process on Stress Corrosion Cracking—Summary of Testing 1984-1985*, EPRI NP-4222 Vol. 5 (January 1987).

48. M. T. Wang, *Corrosion Evaluation of Two Processes for Chemical Decontamination of BWR Structural Materials*, EPRI NP-4356 (December 1985).

49. B. M. Gordon, *Decontamination Guidelines for Materials and Corrosion Concerns in BWRs*, EPRI NP-4749-LD (July 1986).

50. T. K. Odegaard, *Effects of Decontamination and Surface Treatment on the Intergranular Stress Corrosion Cracking of Reactor Materials*, EPRI NP-4777-LD (November 1986).

51. R. A. Speranzini, R. L. Tapping, and D. J. Disney, "Corrosiveness of Decontamination Solutions to Sensitized Type 304 Stainless Steel," *Corrosion* (Houston) **43**, 632-641 (1987).

52. R. Knox, "How Independent Tests Have Eliminated Can-Decon Corrosion Concerns," *Nucl. Eng. Int.* **32**, 48–51 (1987).

53. D. Bradbury, M. G. Segal, R. M. Sellers, T. Swan, and C. J. Wood, *Development of LOMI Chemical Decontamination Technology*, EPRI NP-3177 (July 1983).

54. R. L. Clark and R. L. McDowell, *Corrosion Testing of LOMI Decontamination Reagents*, EPRI NP-3940 (March 1985).

55. D. R. Diercks, "Effect of Decontamination on Life Extension and Aging Considerations," Proc. 15th Water Reactor Safety Information Meeting, NUREG/CP-0091 Vol. 6 (February 1988), pp. 27–41.

56. D. R. Diercks, *Chemical Decontamination and Chemical Cleaning of LWR Components and Possible Interactions with Metallurgical Aging Effects*, NUREG/CR-5180, ANL-88-30 (November 1988).

57. W. E. Ruther, W. K. Soppet, and T. F. Kassner, in *Environmentally Assisted Cracking in Light Water Reactors: Semiannual Report, October 1986–March 1987*, NUREG/CR-4667 Vol. IV, ANL-87-41 (December 1987), pp. 47–53.

58. P. S. Maiya, in *Environmentally Assisted Cracking in Light Water Reactors Semiannual Report April–September 1986*, NUREG/CR-4667 Vol. III, ANL-87-37 (September 1987), pp. 7–26.

59. M. E. Indig and J. E. Weber, "Effects of H_2 Additions on Stress Corrosion Cracking in a Boiling Water Reactor," *Corrosion* (Houston) **41**, 19–30 (1985).

60. W. E. Ruther, W. K. Soppet, and T. F. Kassner, in *Environmentally Assisted Cracking in Light Water Reactors: Annual Report, October 1982–September 1983*, NUREG/CR-3806, ANL-84-36 (June 1984), pp. 101–128.

61. W. E. Ruther, W. K. Soppet, and T. F. Kassner, in *Light-Water-Reactor Safety Materials Engineering Research Programs: Quarterly Progress Report January–March 1985*, NUREG/CR-4490 Vol. 1, ANL-85-75 Vol. 1 (March 1986), pp. 43–48.

62. P. S. Maiya, "A Phenomenological Model for Stress Corrosion Cracking in Types 316NG and 316 Stainless Steel," in *Environmental Degradation of Materials in Nuclear Power Systems-Water Reactors*, NACE, Houston (1986), pp. 12–17 and 53.

63. F. P. Ford, D. T. Taylor, P. L. Andresen, and R. G. Ballinger, *Corrosion-Assisted Cracking of Stainless and Low-Alloy Steels in LWR Environments*, EPRI NP-5064S (February 1987).

64. L. G. Ljungberg, D. Cubicciotti, and M. Trolle, "Materials Behavior in Alternate (Hydrogen) Water Chemistry in the Ringhals-1 Boiling Water Reactor," *Corrosion* (Houston) **42**, 263–271 (1986).

65. L. Frank, W. S. Hazelton, R. A. Herman, V. S. Noonan, and A. Taboada, *Pipe Cracking Experience in Light-Water Reactors*, NUREG-0679 (August 1980), pp. 7-9.

66. PWR Pipe Crack Study Group, *Investigation and Evaluation of Cracking Incidents in Piping in Pressurized Water Reactors*, NUREG-0691 (September 1980), pp. 2-12 to 2-23.

67. A. Goldberg, R. D. Streit, and R. G. Scott, *Evaluation of Cracking in Feedwater Piping Adjacent to Steam Generators in Nine Mile Point Pressurized Water Reactor Plants*, NUREG/CR-1603, UCRL-53000 (October 1980).

68. B. Vyas, C. J. Czajkowski, and J. R. Weeks, "Metallurgical Examination of Cracked Feedwater Pipes from Nine Pressurized Water Reactors," *Nucl. Technol.* **55**, 525-537 (1981).

69. J. F. Enrietto, W. H. Bamford, and D. F. White, "Preliminary Investigation of PWR Feedwater Line Cracking," *Int. J. Pressure Vessel Piping* **9**, 345-358 (1981).

70. C. J. Czajkowski, *Investigation of Shell Crack on the Steam Generators at Indian Point Unit No. 3*, NUREG/CR-3281, BNL-NUREG-51670 (June 1983).

71. J. Hickling and D. Blind, "Strain-Induced Corrosion Cracking of Low-Alloy Steels in LWR Systems — Case Histories and Identification of Conditions Leading to Susceptibility," *Nucl. Eng. Des.* **91**, 305-330 (1986).

72. J. Jansky, D. Blind, and G. Katzenmeier, "Investigation of Piping Failure in the HRD Test Plant under Operational Conditions and the Influence of Oxygen Content," *Nucl. Eng. Des.* **91**, 345-358 (1986).

73. C. J. Czajkowski, "Evaluation of Transgranular Cracking Phenomenon on the Indian Point No. 3 Steam Generator Vessels," *Int. J. Pressure Vessel Piping* **26**, 97-110 (1986).

74. H. Choi, F. H. Beck, Z. Szklarska-Smialowska, and D. D. Macdonald, "Stress Corrosion Cracking of ASTM A508 Cl 2 Steel in Oxygenated Water at Elevated Temperatures," *Corrosion (Houston)* **38**, 136-144 (1982).

75. T. Mizuno, S. Pednekar, Z. Szklarska-Smialowska, and D. D. Macdonald, "Corrosion and Stress Corrosion Cracking of Carbon Steel in Oxygenated, High-Purity Water at Elevated Temperatures," in *Environmental Degradation of Materials in Nuclear Power Systems-Water Reactors*, Proc. Int. Symp., Myrtle Beach, SC, August 22-25, 1983, NACE, Houston (1984), pp. 395-422.

76. C. J. Czajkowski, *Constant Extension Rate Testing of SA302 Grade B Material in Neutral and Chloride Solutions*, NUREG/CR-3614, BNL-NUREG-51736 (February 1984).

77. P. Hurst, D. A. Appleton, P. Banks and A. S. Raffel, "Slow Strain Rate Stress Corrosion Tests on A508–III and A533B in Deionized and PWR Water at 563K," *Corros. Sci.* **25**, 651–671 (1985).

78. J. Congleton, T. Shoji, and R. N. Parkins, "The Stress Corrosion Cracking of Reactor Pressure Vessel Steel in High Temperature Water," *Corros. Sci.* **25**, 633–650 (1985).

79. J. Kuniya, I. Masaoka, R. Sasaki, H. Itoh, and T. Okazaki, "Stress Corrosion Cracking Susceptibility of Low–Alloy Steels Used for Pressure Vessel Steels Used for Reactor Pressure Vessel in High–Temperature Oxygenated Water," *Trans. ASME J. Pressure Vessel Technol.* **107**, 431–435 (1985).

80. K. Klemetti and H. Hanninen, "Effect of Electrochemical Potential on Stress Corrosion Cracking of Steel A508 in BWR Environment," in *Environmental Degradation of Materials in Nuclear Power Systems–Water Reactors*, Proc. 2nd Int. Symp., Monterey, CA, September 9–12, 1985, NACE, Houston (1986), pp. 70–76.

81. E. Lenz and N. Wieling, "Strain–Induced Cracking of Low–Alloy Steels in LWR Systems — Interpretation of Susceptibility by Means of a Three Dimensional (T, ε, Dissolved Oxygen) Diagram," *Nucl. Eng. Des.* **91**, 331–344 (1986).

82. T. Shoji, H. Nakajama, H. Tsuji, H. Takahashi, and T. Kondo, "Effect of Microstructure and Strength of Low–Alloy Steels on Cyclic Crack Growth in High–Temperature Water," in *Corrosion Fatigue: Mechanics, Metallurgy, Electrochemistry, and Engineering*, ASTM STP 801, T. W. Crooker and B. N. Leis, eds., ASTM, Philadelphia (1983), pp. 256–286.

83. K. Torronen and M. Kemppainen, "Fractography and Mechanisms of Environmentally Enhanced Fatigue Crack Propagation of a Reactor Pressure Vessel Steel," in *Corrosion Fatigue: Mechanics, Metallurgy, Electrochemistry, and Engineering*, ASTM STP 801, T. W. Crooker and B. N. Leis, eds., ASTM, Philadelphia (1983), pp. 287–318.

84. D. Weinstein, *BWR Environmental Cracking Margins for Carbon Steel Piping, Final Report*, EPRI–2406 (May 1982).

85. C. Amzallag, J. L. Bernard, and G. Slama, "Effect of Loading on Metallurgical Parameters on the Fatigue Crack Growth Rates of Pressure Vessel Steels in Pressurized Water Reactor Environment," in *Environmental Degradation of Materials in Nuclear Power Systems–Water Reactors*, Proc. Int. Symp., Myrtle Beach, SC, August 22–25, 1983, NACE, Houston (1984), pp. 727–745.

86. W. H. Bamford, "Environmental Cracking of Pressure Boundary Materials and the Importance of Metallurgical Considerations," in *Aspects of Fracture Mechanics in Pressure Vessels and Piping*, ASME PVP–58, S. S. Palusamy and S. G. Sampath, eds., New York (1982), pp. 209–228.

87. P. M. Scott and A. E. Truswell, "Corrosion Fatigue Crack Growth in Reactor Pressure Vessel Steels in PWR Primary Water," in *Aspects of Fracture Mechanics in Pressure*

Vessels and Piping, ASME PVP–58, S. S. Palusamy and S. G. Sampath, eds., New York (1982), pp. 271–301.

88. W. H. Cullen, "Effects of Loading Rate, Waveform, and Temperature on Fatigue Crack Growth Rates of RPV Steels," in *Aspects of Fracture Mechanics in Pressure Vessels and Piping*, ASME PVP–58, S. S. Palusamy and S. G. Sampath, eds., New York (1982), pp. 303–312.

89. J. Y. Park, in *Environmentally Assisted Cracking in Light–Water–Reactors: Semiannual Report October 1986–March 1987*, NUREG/CR–4667 Vol. IV, ANL–87–41 (December 1987), p. 54.

90. P. M. Scott, A. E. Truswell, and S. G. Bruce, "Corrosion Fatigue of Pressure Vessel Steels in PWR Environment–Influence of Steel Sulfur Content, " *Corrosion (Houston)* **40**, 350–357 (1984).

91. J. H. Bulloch, "The Effect of Sulfide Distribution and Morphology on Environmentally Assisted Cracking Behavior of Ferritic Reactor Pressure Vessel Materials," in *Proc. 3rd Int. Symp. on Environmental Degradation of Materials in Nuclear Power Systems–Water Reactors*, G. J. Theus and J. R. Weeks, eds., American Nuclear Society, LaGrange Park, IL (1988), pp. 261–268.

Distribution for NUREG/CR-4667 Vol. V (ANL-88-32)

Internal:

W. J. Shack (30)
TIS File (3)
ANL Libraries (2)
ANL Patent File
ANL Contract File

External:

NRC, for distribution per R5 (315)
Manager, Chicago Operations Office, DOE
Materials and Components Technology Division Review Committee:
- Dr. Peter Alexander, Director of Engineering, Instrumentation Products, Combustion Engineering, 400 West Avenue, Rochester, New York 14611
- Dr. Stanley J. Green, Electric Power Research Institute, 3412 Hillview Avenue, Palo Alto, CA 94303
- Dr. Robert A. Greenkorn, Purdue University, Hovde Hall, Room 222, West Lafayette, IN 47907
- Dr. Leslie J. Jardine, Bechtel National, Inc., 45 Fremont Street, 11/B33, San Francisco, CA 94105
- Dr. Che-Yu Li, Department of Materials Science and Engineering, Cornell University, Bard Hall, Ithaca, NY 14853
- Dr. Roger E. Scholl, URS/John A. Blume & Associates, 150 Fourth Street, Sixth Floor, San Francisco, CA 94103
- Dr. P. G. Shewmon, Dept. of Metallurgical Engineering, Ohio State University, 116 W. 19th Avenue, Columbus, OH 43210
- Dr. Richard Smith, EPRI NDE Center, 1300 Harris Blvd., Box 217097, Charlotte, NC 28213

P. L. Andresen, General Electric Corporate Research and Development, Schenectady, NY 12301
W. H. Bamford, Structural Materials Engineering, Westinghouse Electric Corp., WNES, Box 355, Pittsburgh, PA 15230
R. M. Crawford, Fluor-Danial Corp., 200 W. Monroe St., Chicago, IL 60606
D. Cubicciotti, Electric Power Research Inst., P. O. Box 10412, Palo Alto, CA 94303
W. H. Cullen, Materials Engineering Assoc., Inc., 9700 B. George Palmer Highway, Lanham, MD 20706
J. C. Danko, U. Tennessee, Knoxville, TN 37996-2000
R. Duncan, Combustion Engineering, Inc., P. O. Box 500, Windsor, CT 06095
M. Fox, APTECH, 1257 Elko Drive, Sunnyvale, CA 94089
Y. S. Garud, S. Levy, Inc., 1901 S. Bascom Ave., Campbell, CA 95008
F. Garzarolli, KWU, Hammerbackerstr. 12+14, Postfac:3220, 8520 Erlangen, West Germany
B. M. Gordon, General Electric Co., 175 Curtner, San Jose, CA 95125
S. D. Harkness, Bettis Atomic Power Laboratory, P. O. Box 79, West Mifflin, PA 15122
D. Harrison, NE42 USDOE, 19901 Germantown Road, Germantown, MD 20874
M. E. Indig, General Electric Co., P. O. Box 460, Pleasanton, CA 94566
H. S. Isaacs, Brookhaven National Laboratory, Upton, NY 11973
R. H. Jones, Battelle Pacific Northwest Lab., P. O. Box 999, Richland, WA 99352
J. N. Kass, Lawrence Livermore National Lab., Livermore, CA 94550
L. Ljungberg, ASEA-ATOM, Box 53, S-721 04, Vasteras, Sweden
C. D. Lundin, U. Tennessee, Knoxville, TN 37996-2200
D. D. Macdonald, SRI International, 333 Ravenswood Ave., Menlo Park, CA 94025

H. Metha, General Electric Co., 175 Curtner, San Jose, CA 95125
R. A. Oriani, U. Minnesota, Minneapolis, MN 55455
S. Ranganath, General Electric Co., 175 Curtner, San Jose, CA 95125
E. J. Rowley, Commonwealth Edison Co., P. O. Box 767, Chicago, IL 60690
P. M. Scott, UKAEA AERE-Materials Development Division, Harwell, Didcot, OXll ORA, UK
S. Smialowska, Dept. of Metallurgical Engineering, Ohio State U., Columbus, OH 43210
D. M. Stevens, Lynchburg Research Center, Babcock & Wilcox Co., P. O. Box 239, Lynchburg, VA 24505
W. A. Van Der Sluys, Research & Development Division, Babcock & Wilcox Co., 5162 Beeson St., Alliance, OH 44601
E. Venerus, Knolls Atomic Power Laboratory, P. O. Box 1072, Schenectady, NY 12301
J. R. Weeks, Brookhaven National Lab., Upton, NY 11973
A. W. Zeuthen, Long Island Lighting Co., P. O. Box 618, Wading River, NY 11792.